nature portfolio

https://doi.org/10.1038/s41586-025-08835-0

Supplementary information

Histone H1 deamidation facilitates chromatin relaxation for DNA repair

In the format provided by the authors and unedited

Supplementary Figure 1: Uncropped immunoblots from Figures.

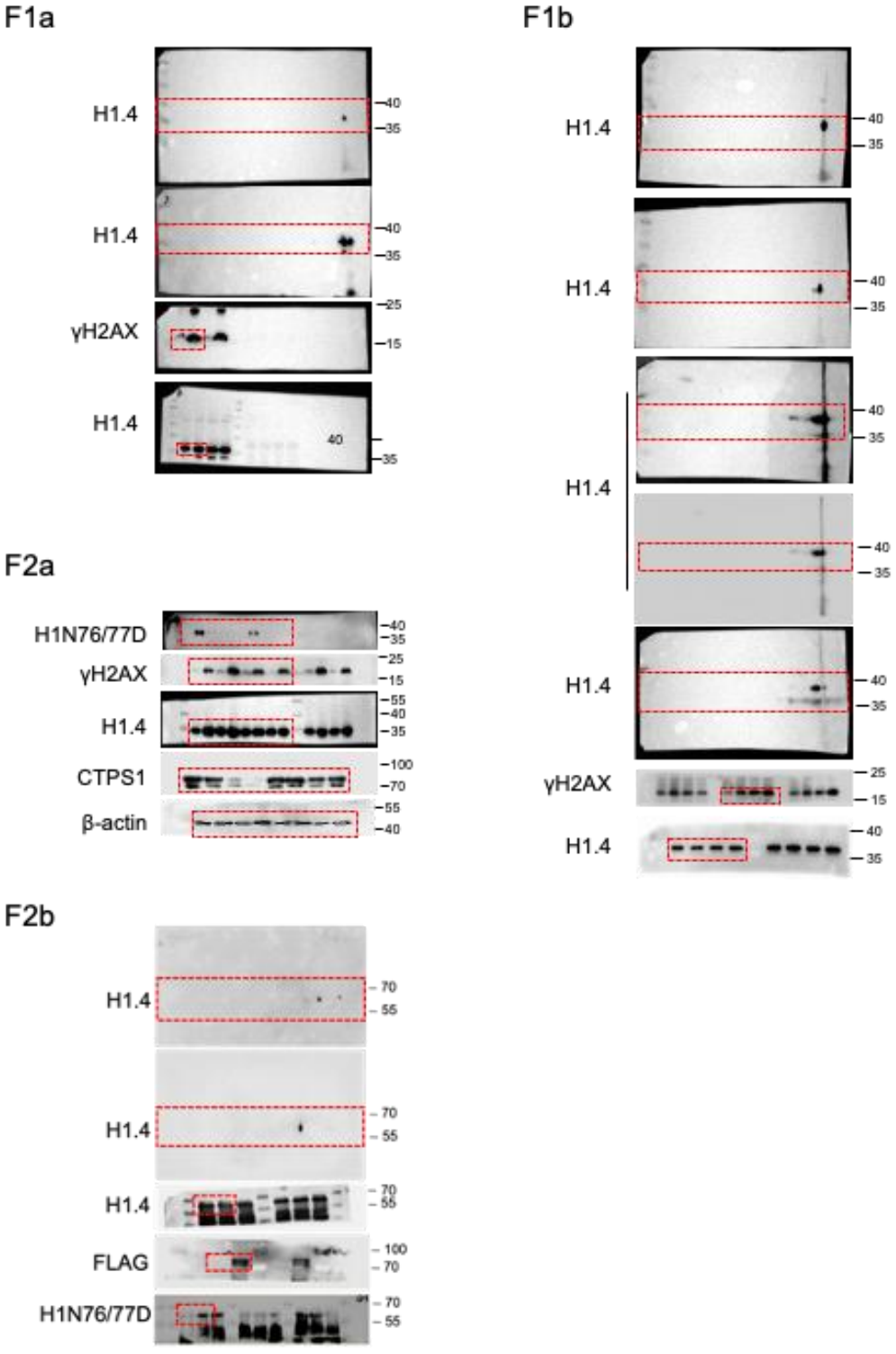

The loading control actin was run on the different gels

F3a

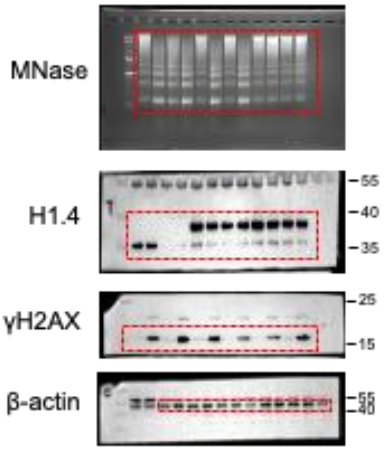

F3b

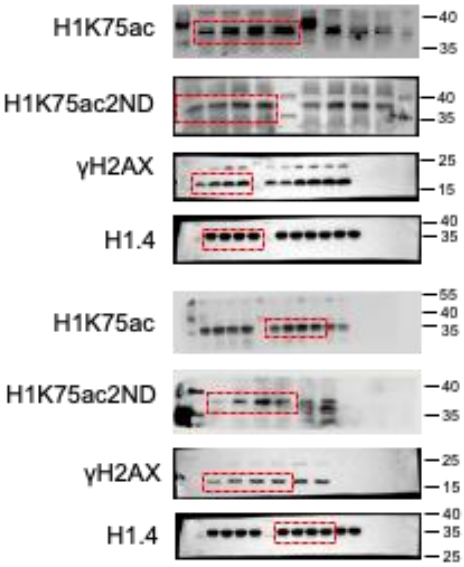

F3c

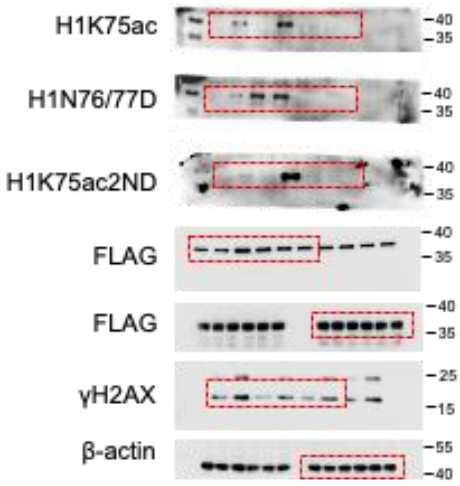

The loading control actin was run on the different gels

F4a

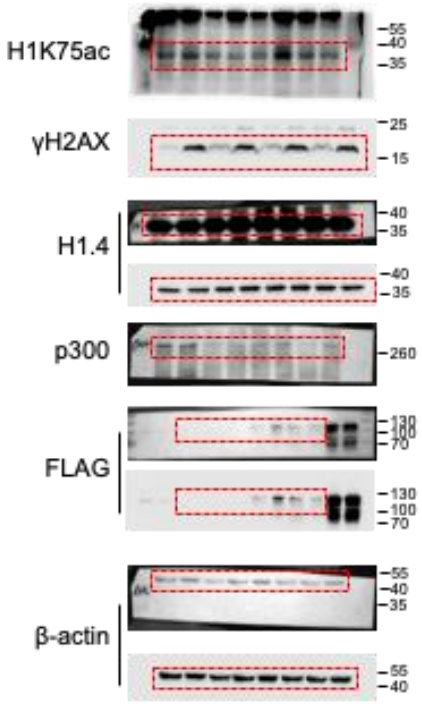

F4b

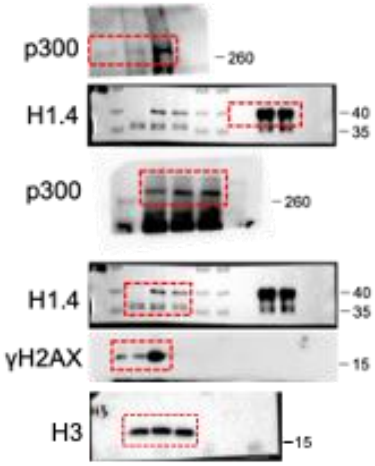

F4c

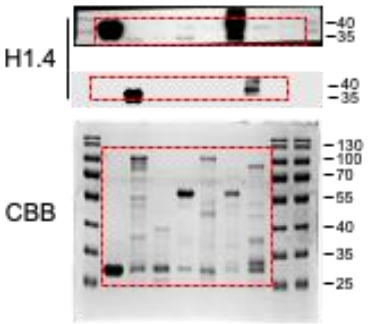

F4d

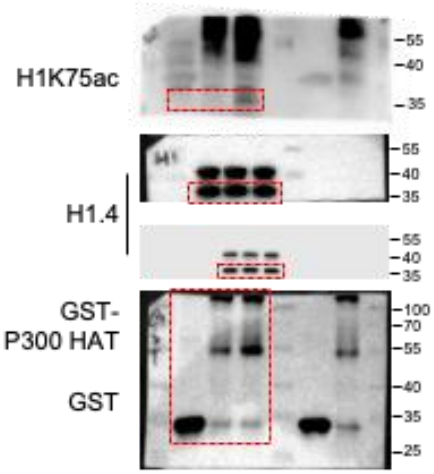

F4e

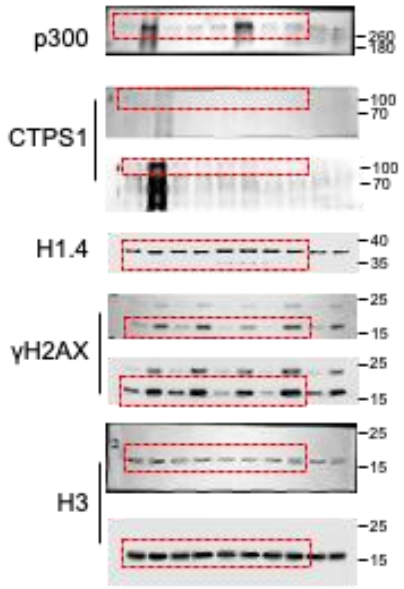

The loading control actin was run on the different gels

F4h

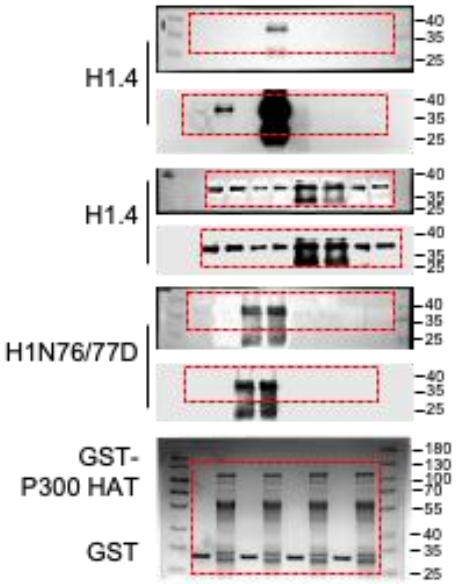

F5a

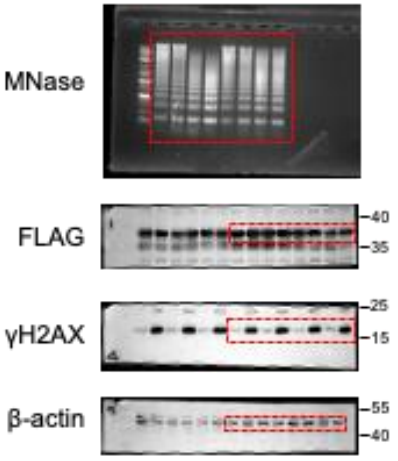

F5d

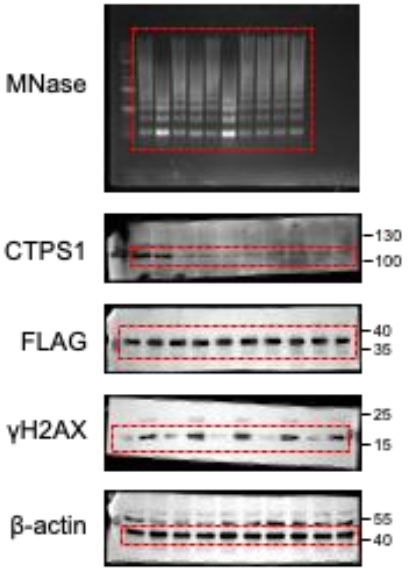

The loading control actin was run on the different gels

ED-F1a

ED-F1b

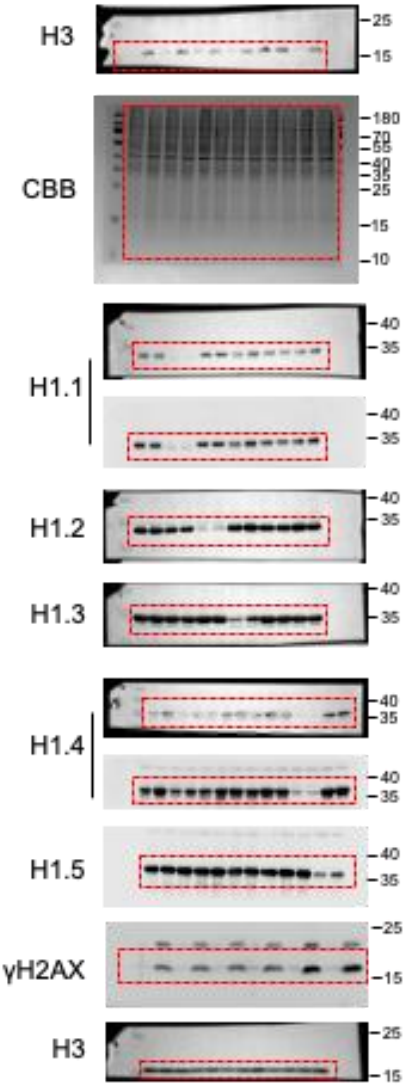

ED-F1c

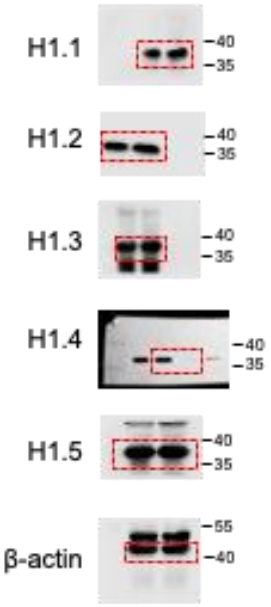

ED-F1d

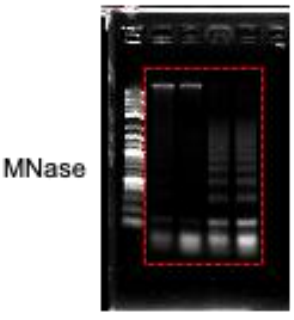

The loading control actin was run on the different gels

ED-F1e

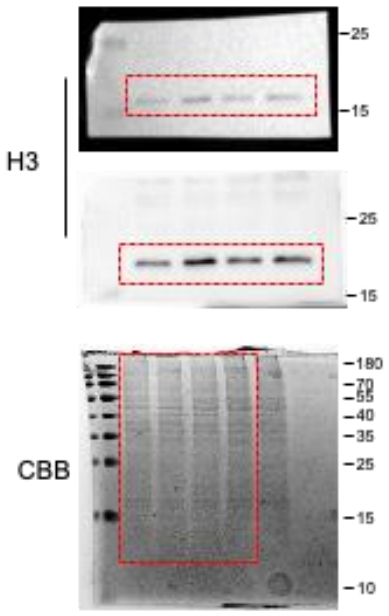

ED-F1f

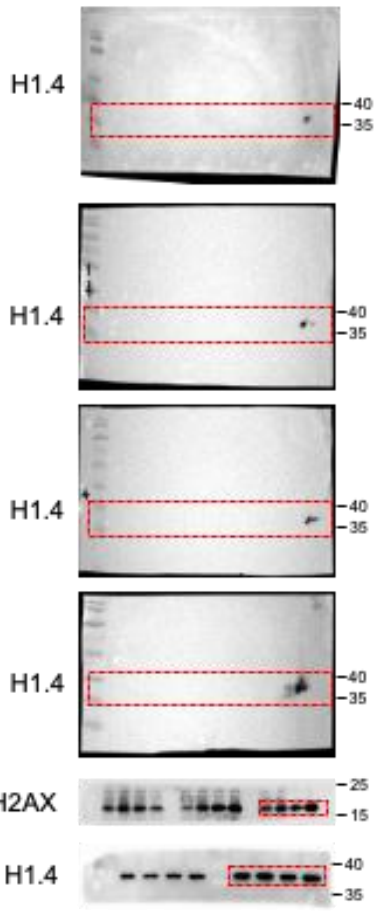

ED-F1g

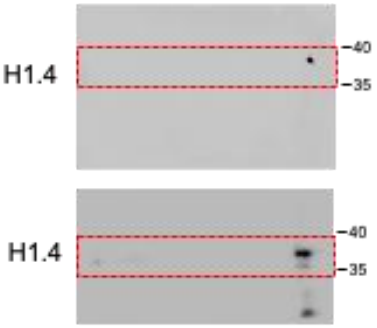

The loading control actin was run on the different gels

ED-F1h

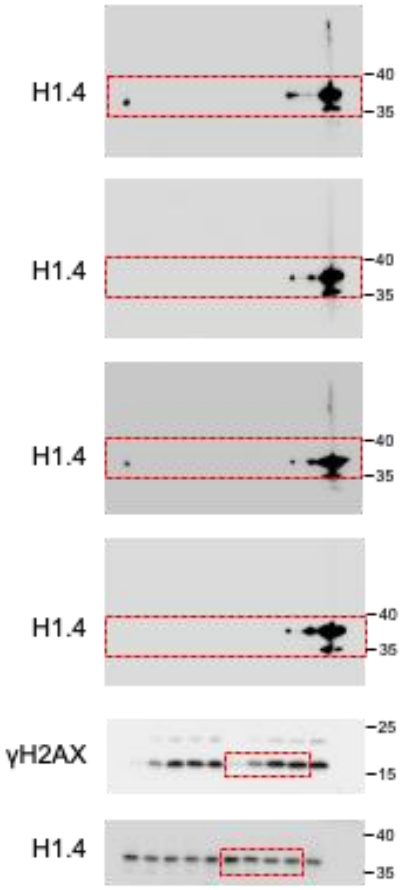

ED-F1l

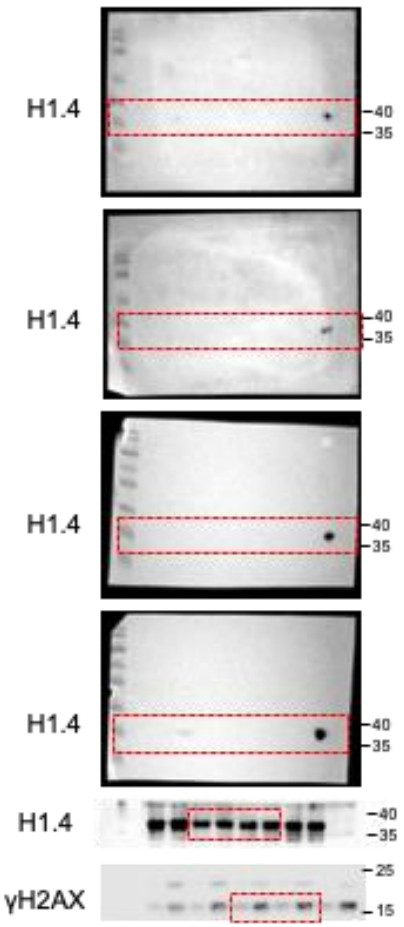

The loading control actin was run on the different gels

ED-F2a

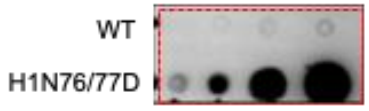

ED-F2c

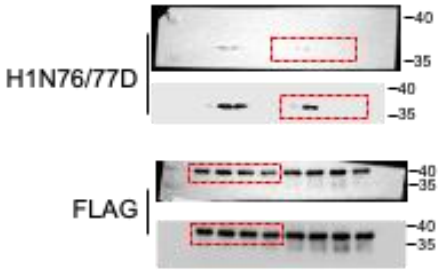

ED-F2d

ED-F2f

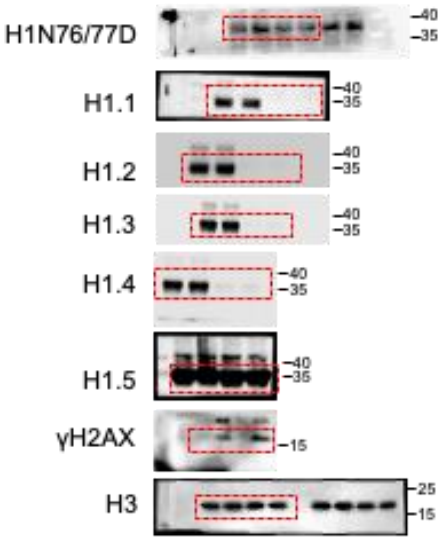

ED-F2g

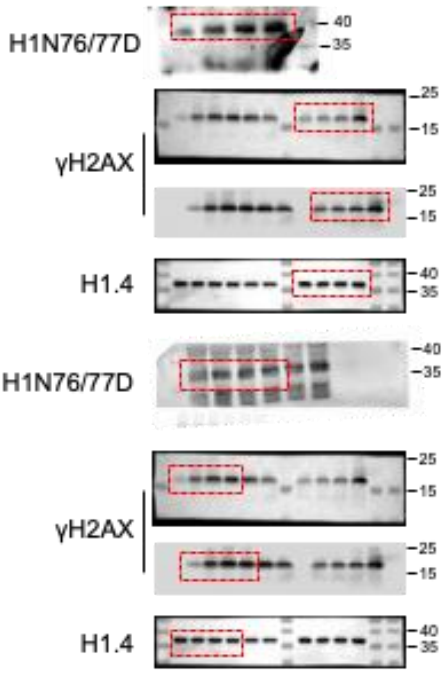

The loading control actin was run on the different gels

ED-F2h

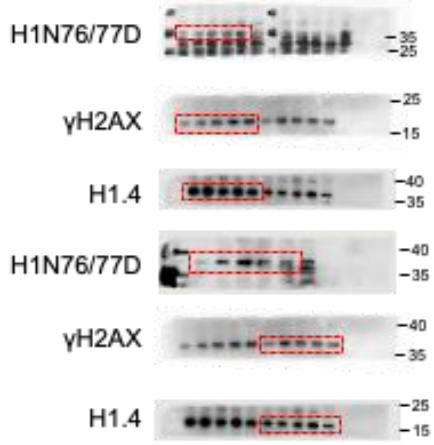

ED-F2k

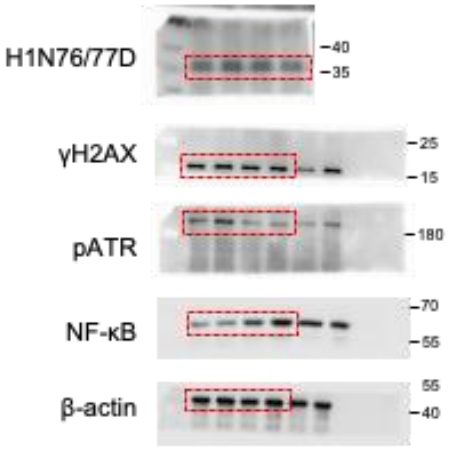

ED-F2j

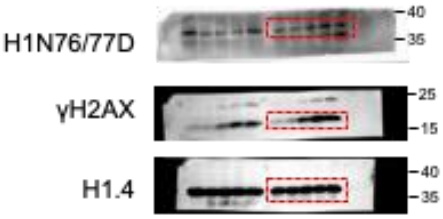

The loading control actin was run on the different gels

ED-F3a

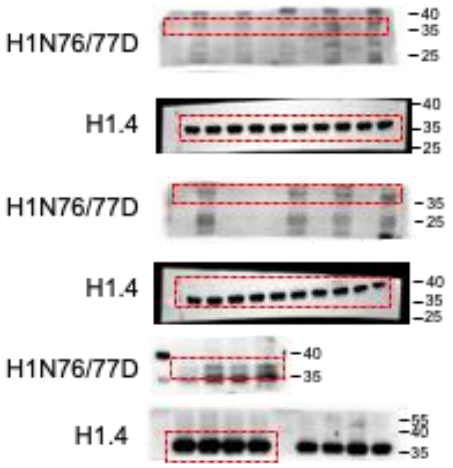

ED-F3b

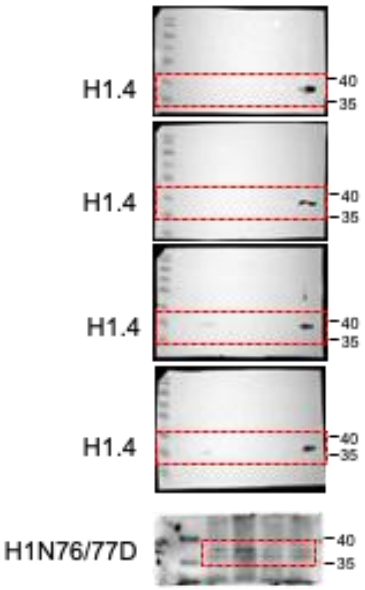

ED-F3c

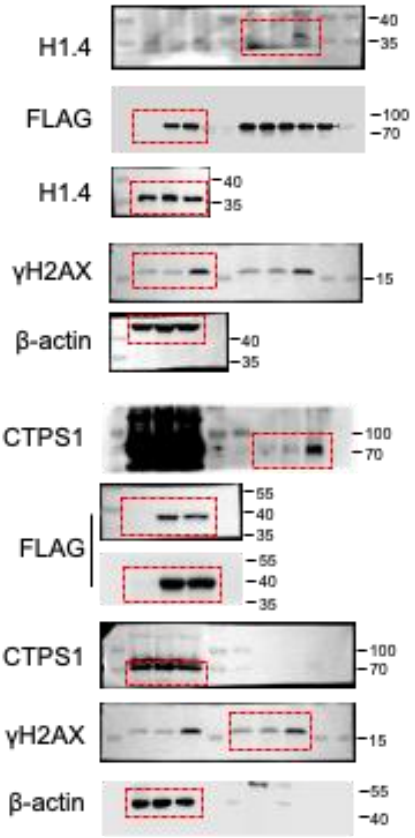

ED-F3d

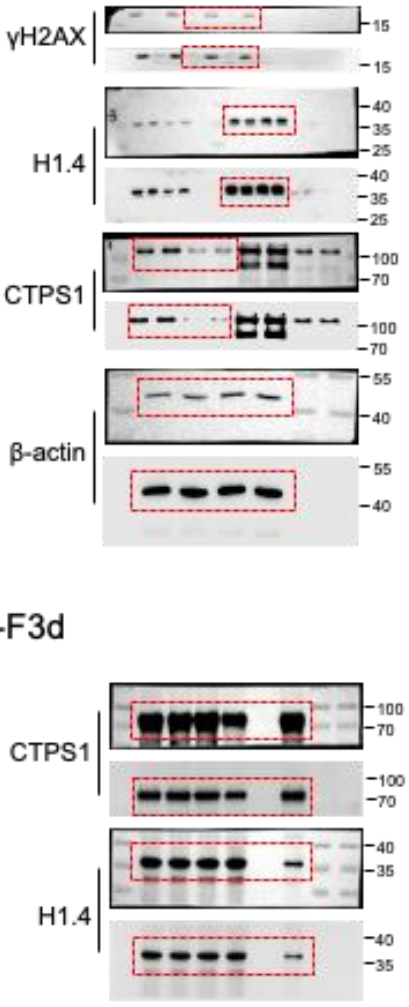

The loading control actin was run on the different gels

ED-F3e

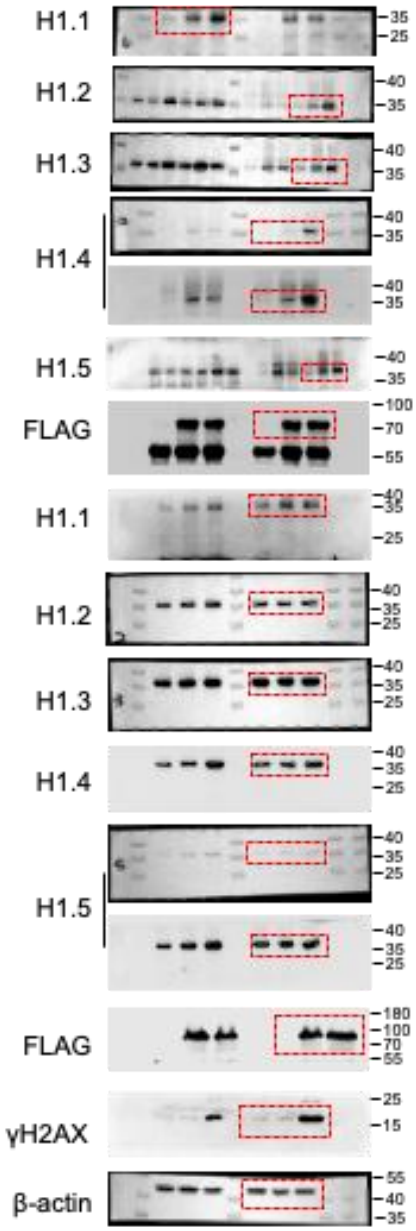

ED-F3f

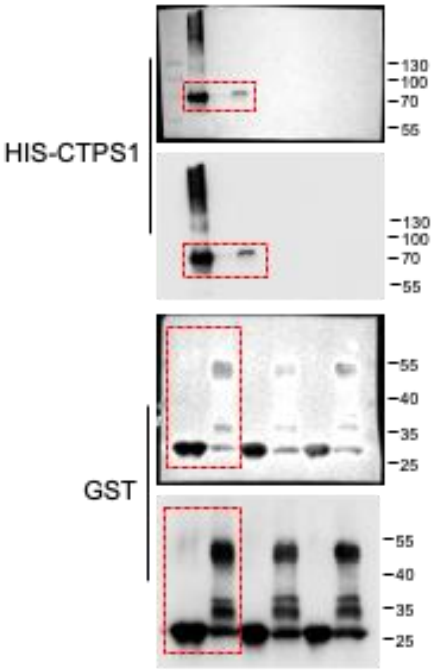

ED-F3g

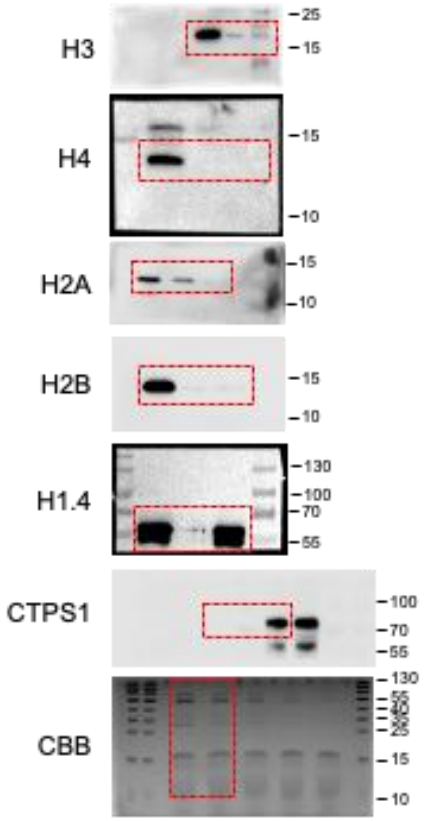

The loading control actin was run on the different gels

ED-F3i

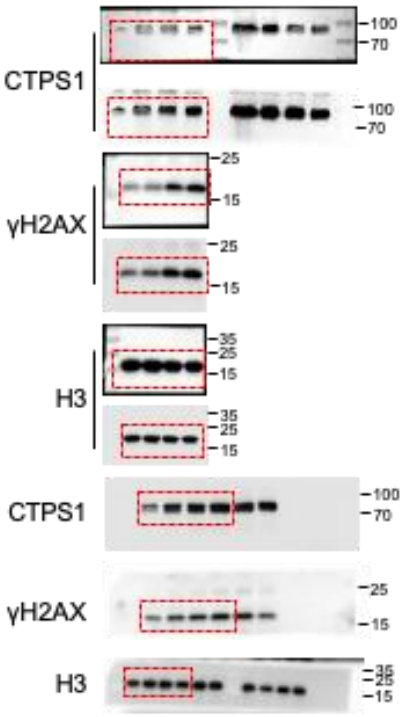

ED-F3h

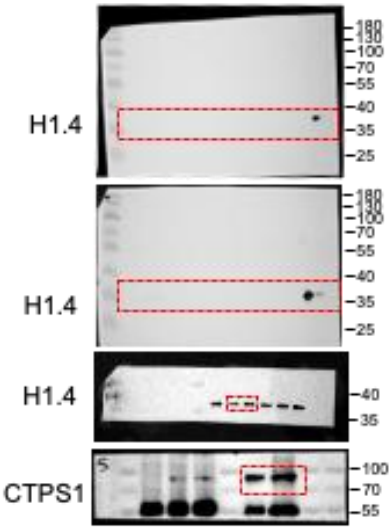

ED-F3j

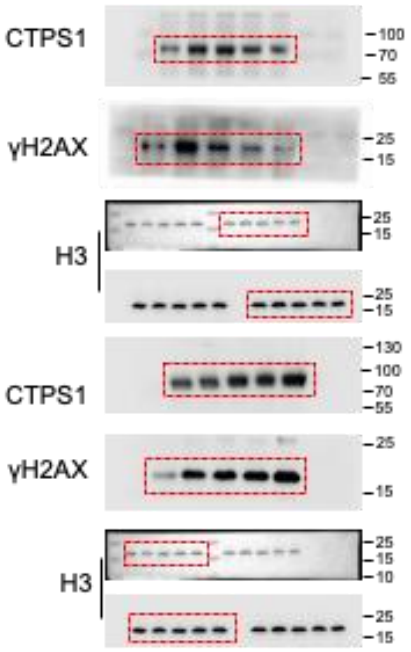

ED-F3n

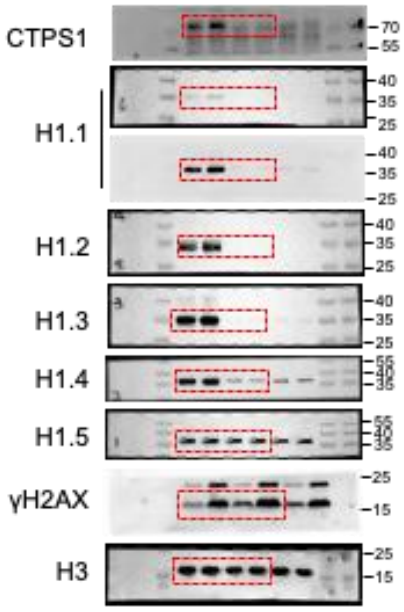

ED-F4h

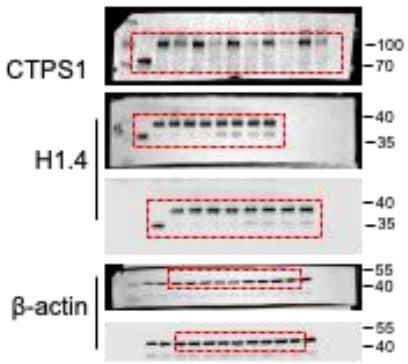

The loading control actin was run on the different gels

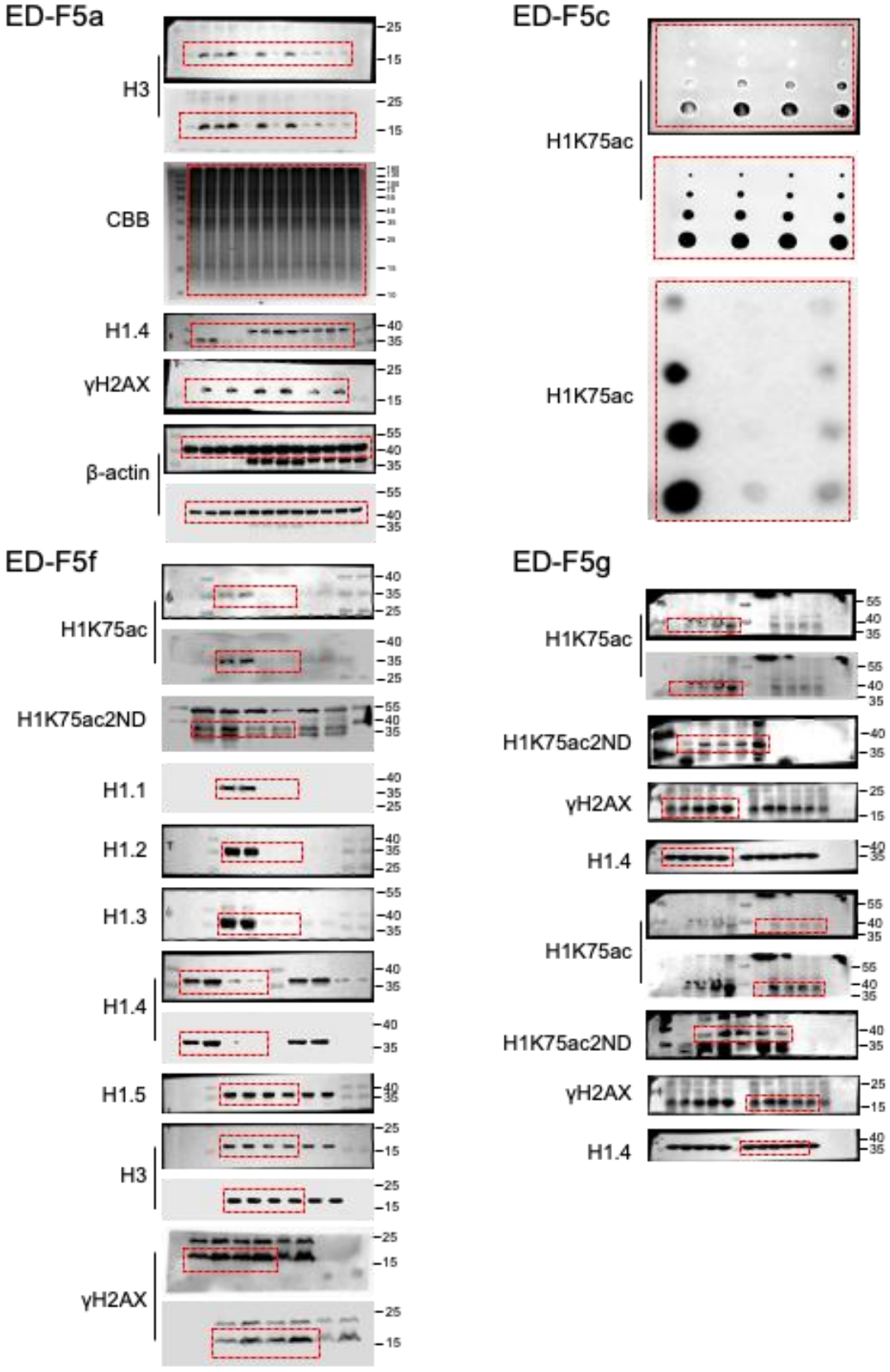

The loading control actin was run on the different gels

ED-F6a

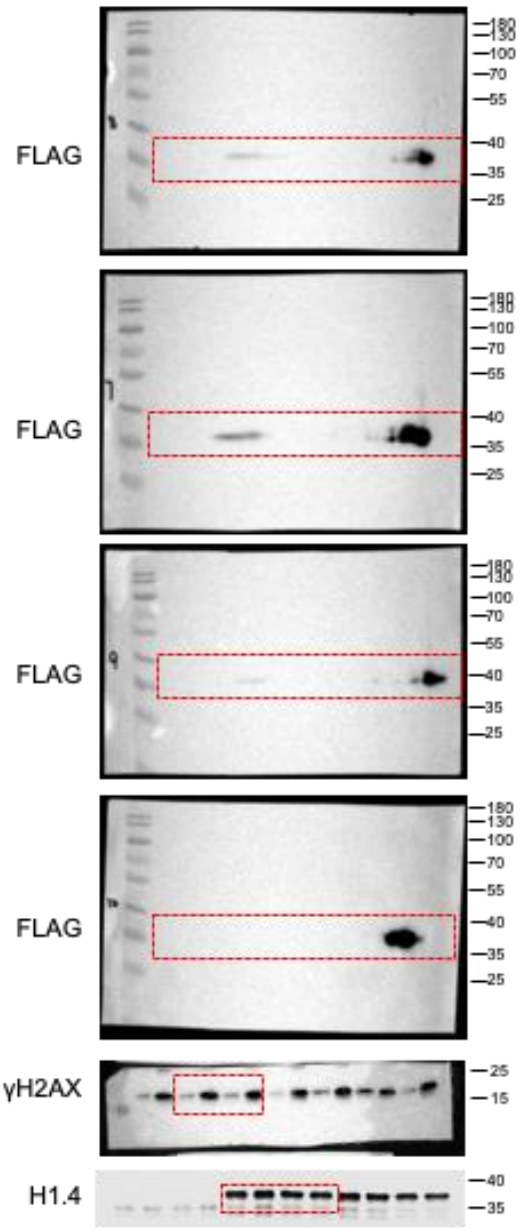

ED-F6b

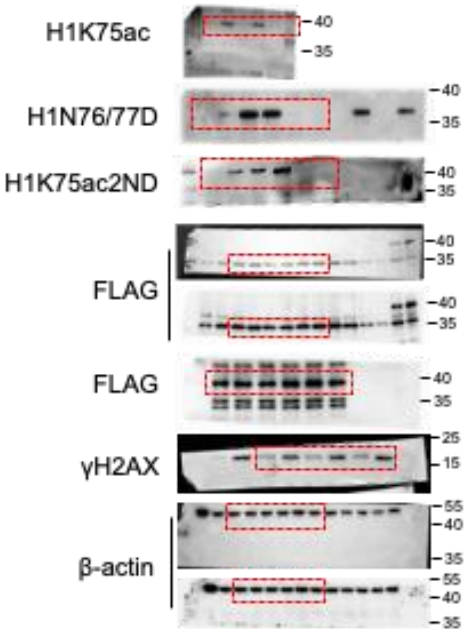

ED-F6c

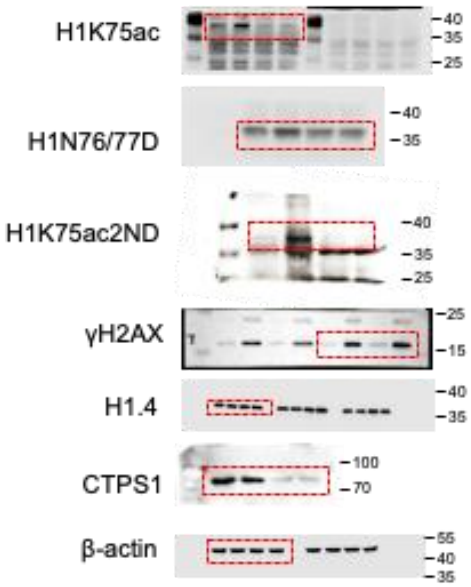

The loading control actin was run on the different gels

ED-F7a

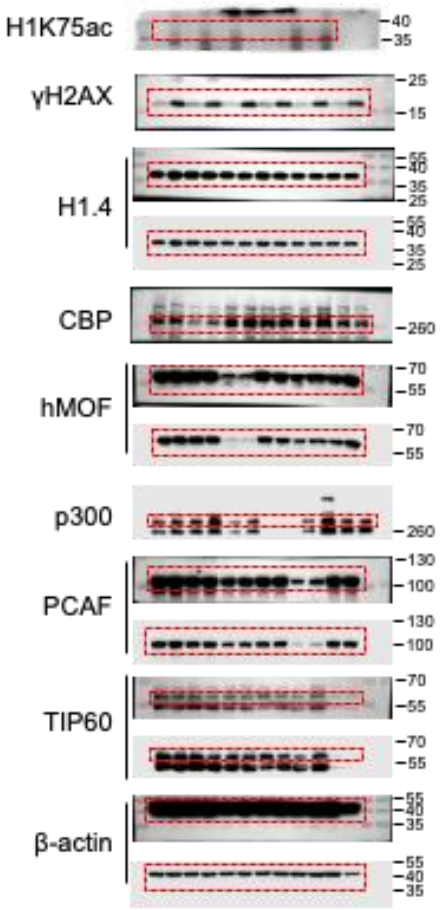

ED-F7b

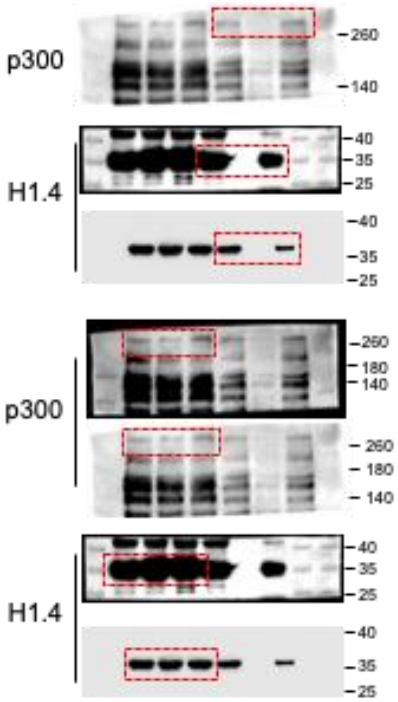

ED-F7c

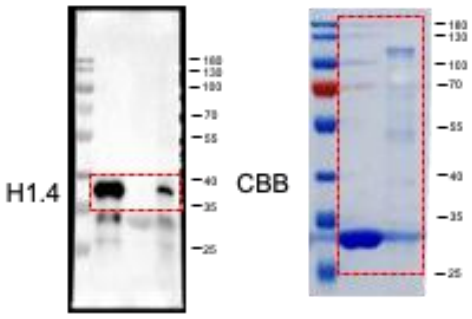

The loading control actin was run on the different gels

ED-F7d

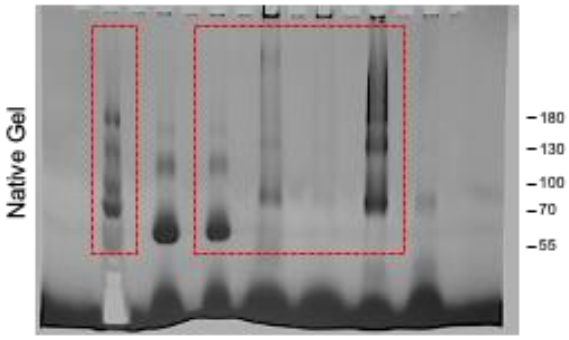

ED-F7f

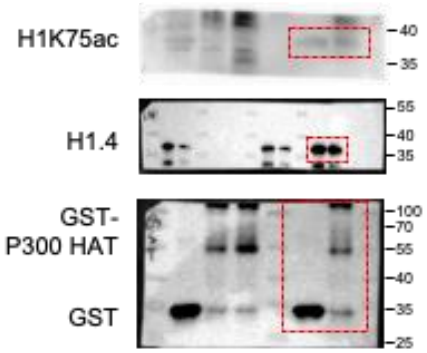

ED-F8b

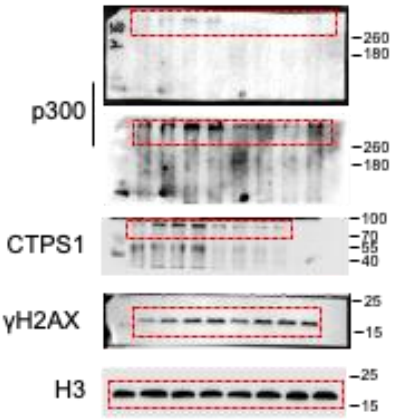

ED-F8c

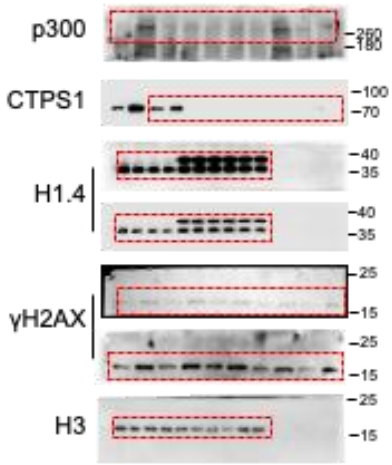

The loading control actin was run on the different gels

ED-F8d

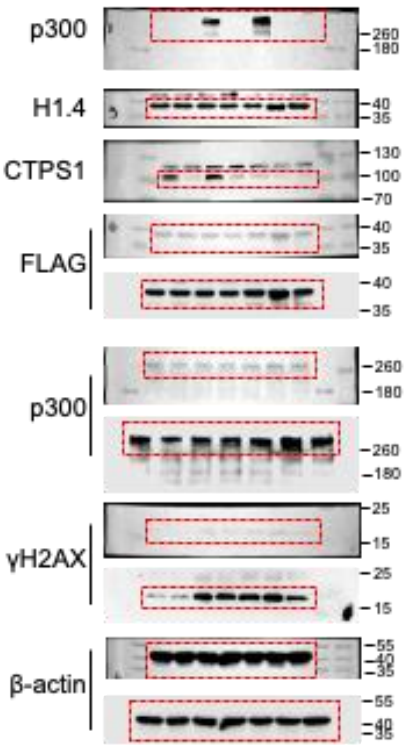

ED-F8e

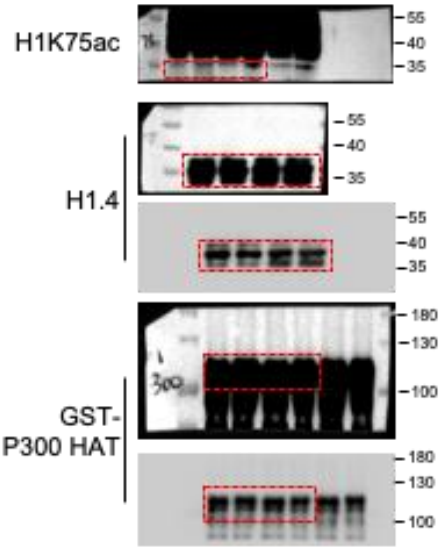

ED-F8g

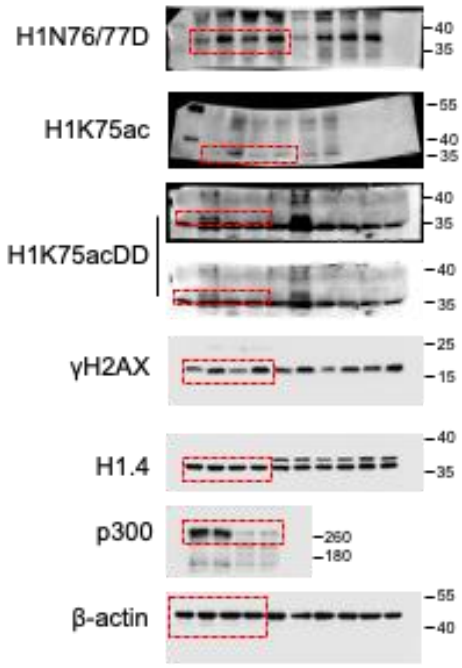

ED-F8h

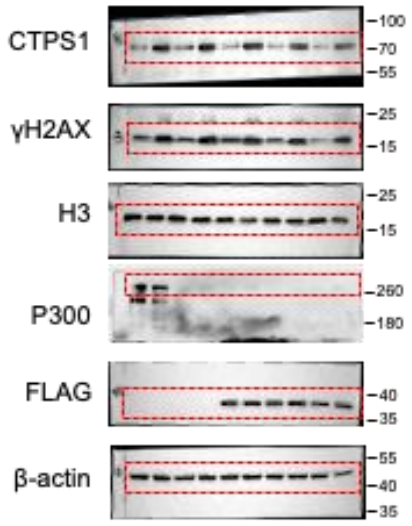

The loading control actin was run on the different gels

ED-F8i

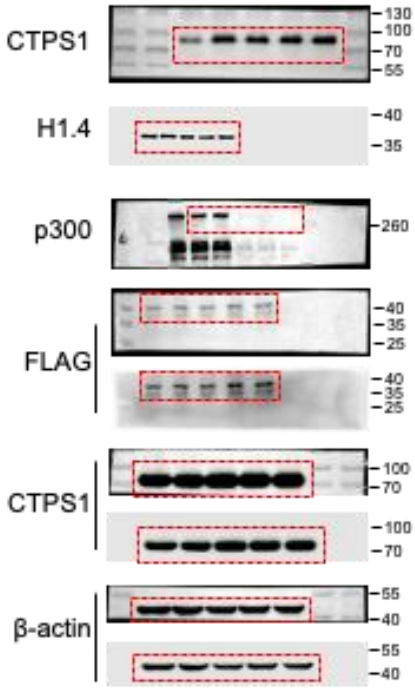

ED-F9a

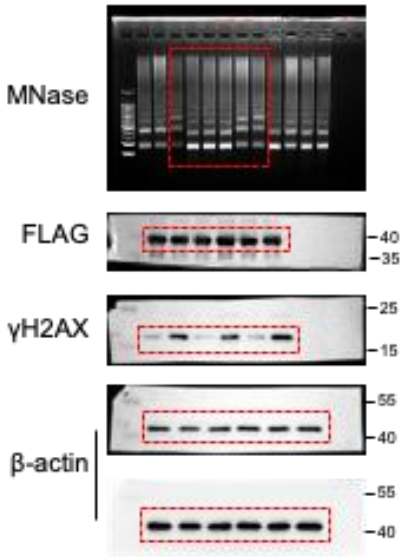

The loading control actin was run on the different gels

ED-F9b

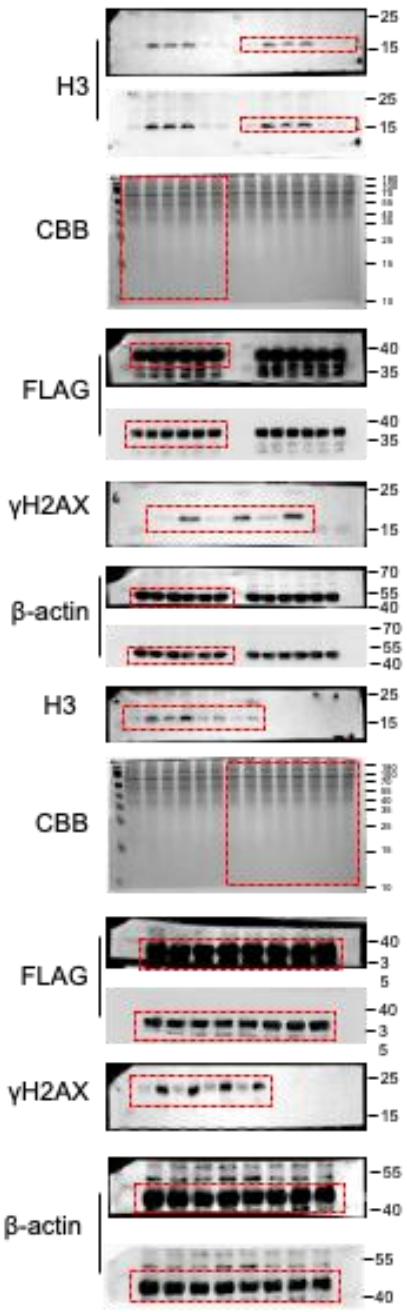

ED-F9c

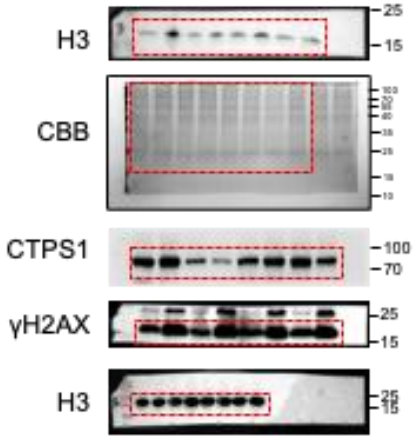

ED-F9d

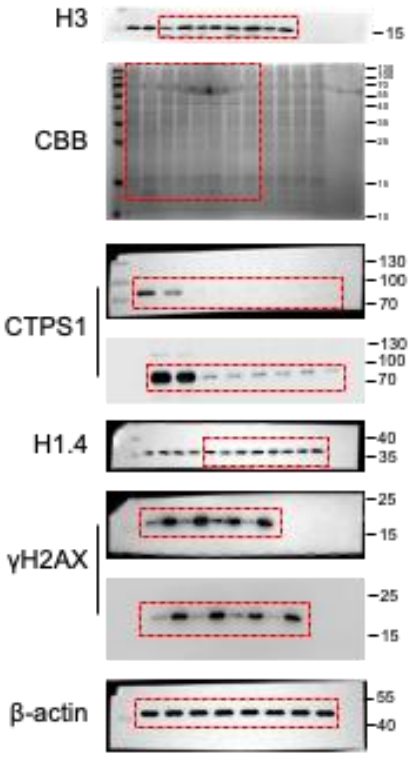

The loading control actin was run on the different gels

ED-F9f

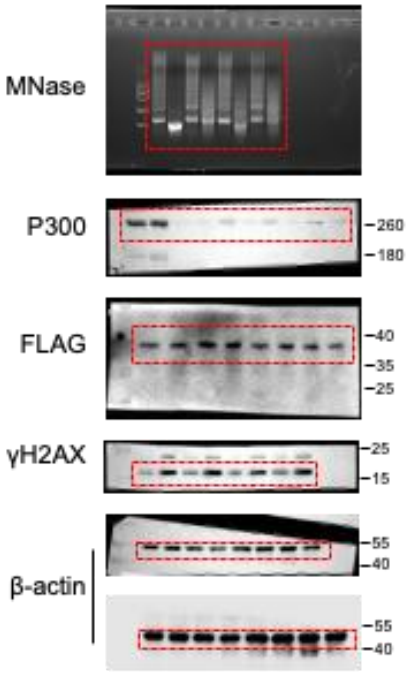

ED-F10i

ED-F10l

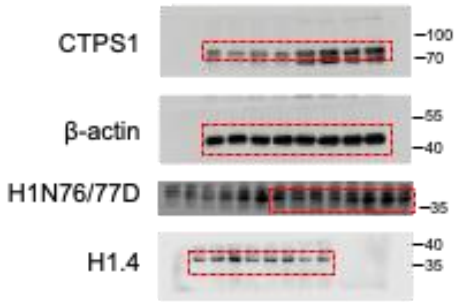

SF3a

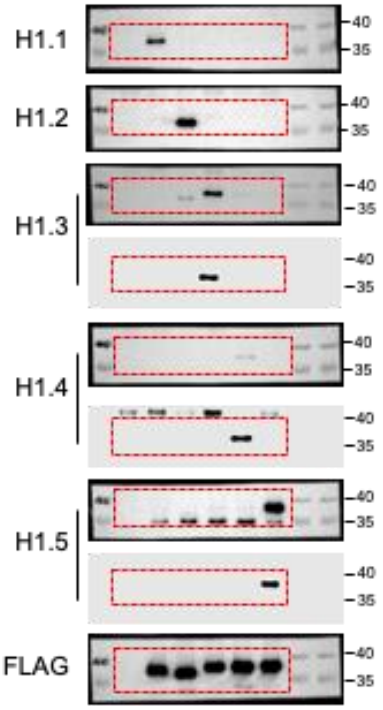

SF4a

The loading control actin was run on the different gels

SF5a

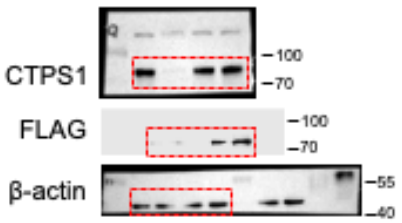

SF5d

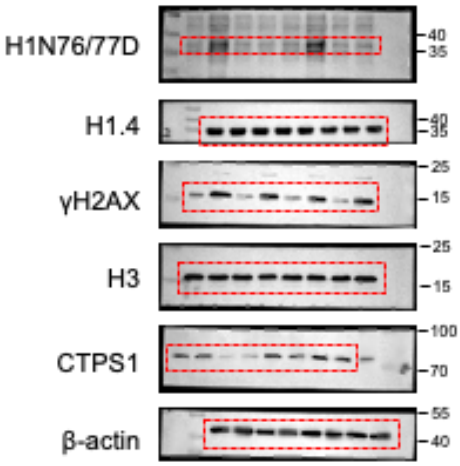

SF5f

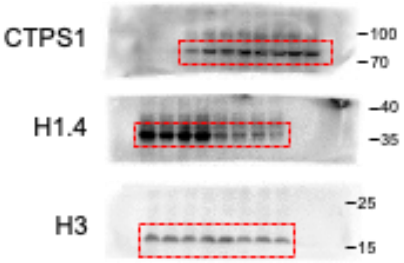

SF5i

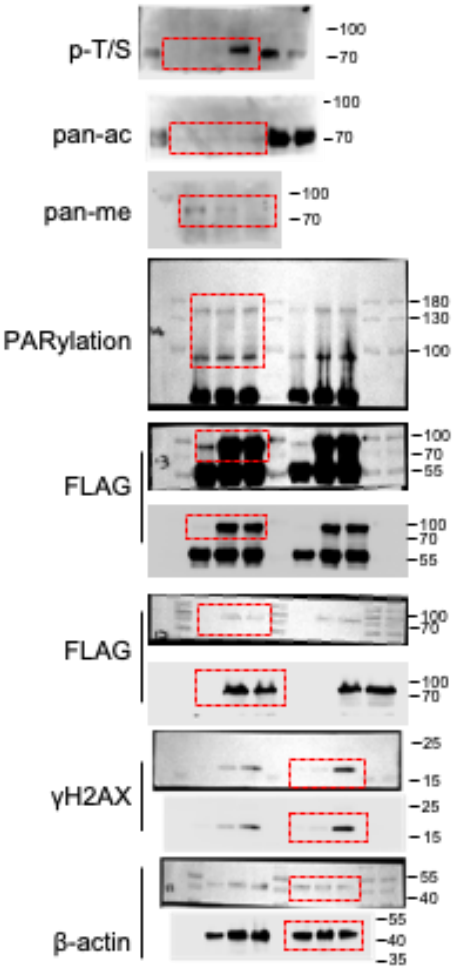

The loading control actin was run on the different gels

SF6c

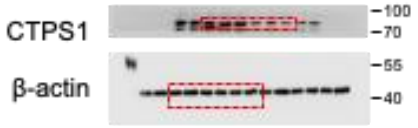

SF6d

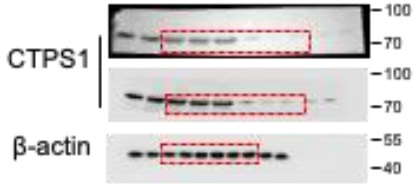

SF6f

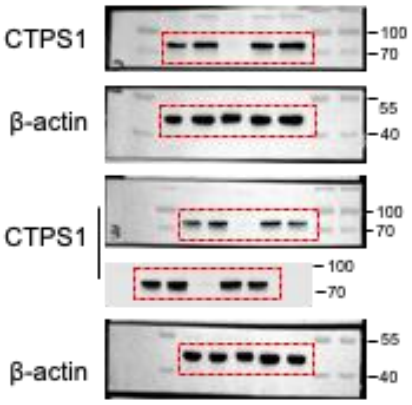

SF6h

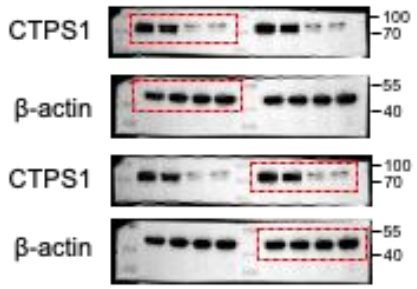

SF7e

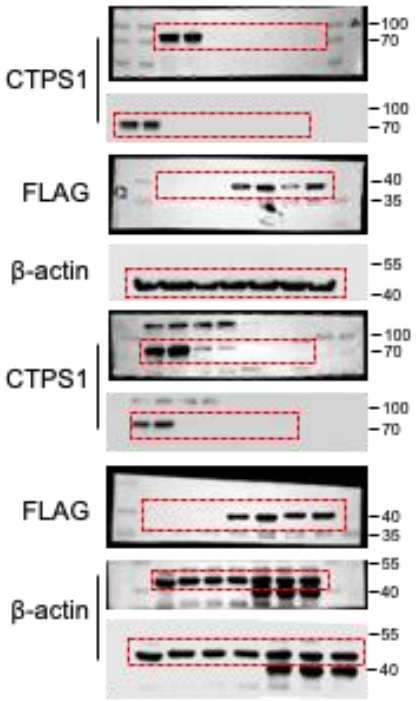

SF9b

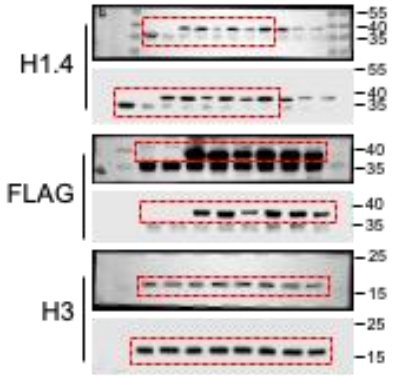

The loading control actin was run on the different gels

SF10d

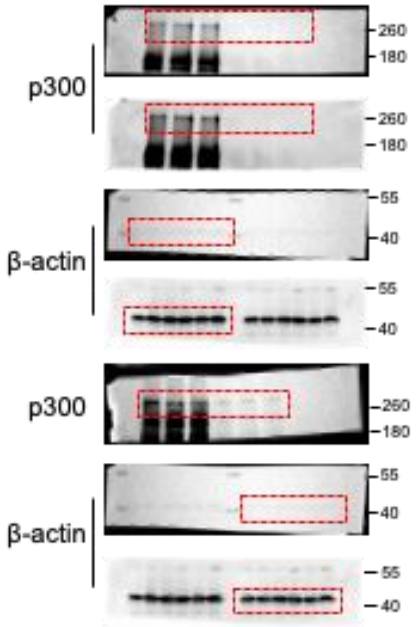

SF10f

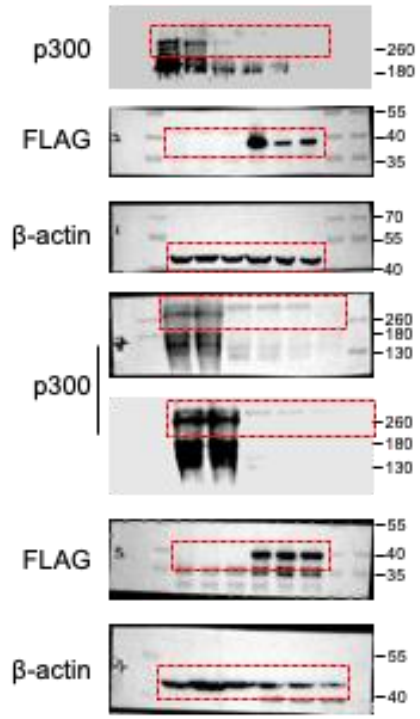

SF11b

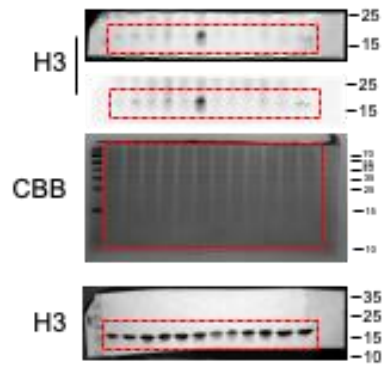

SF11c

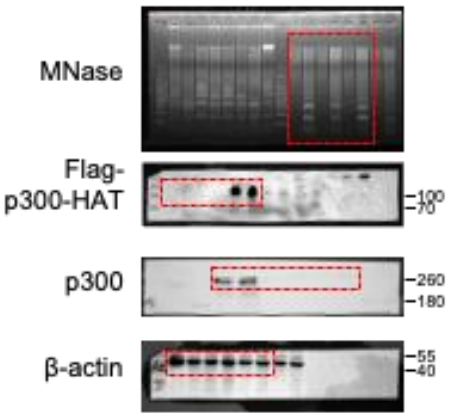

The loading control actin was run on the different gels

SF11e

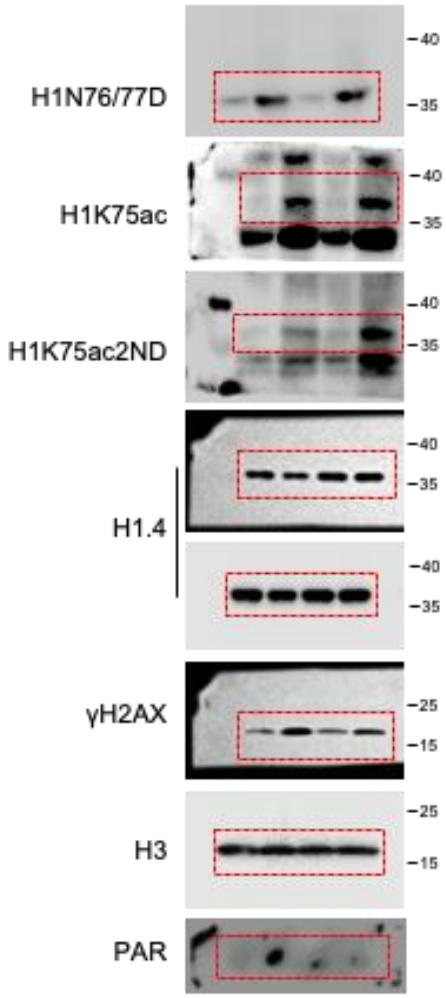

SF11f

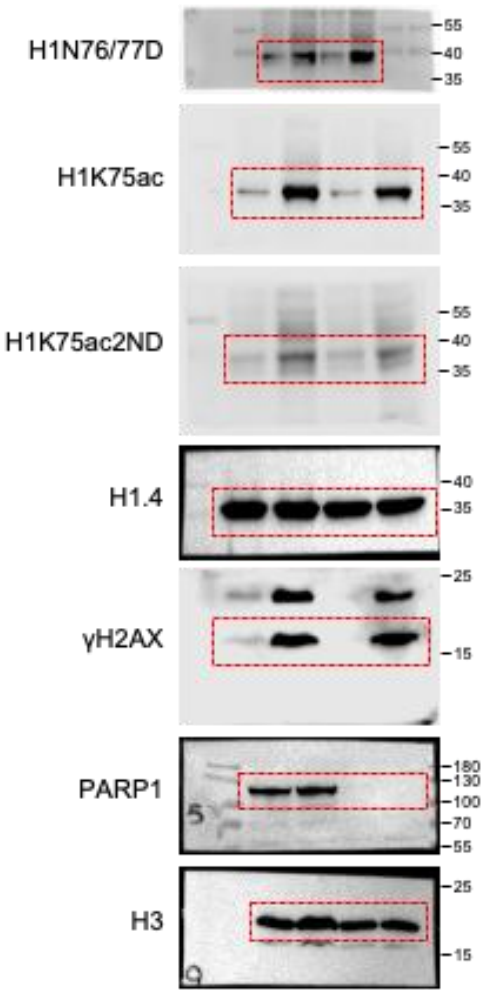

SF12i

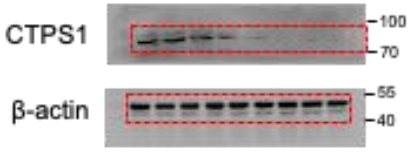

SF12k

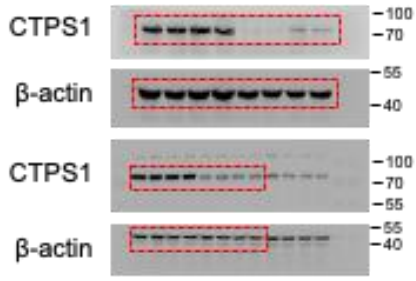

SF13d

SF13e

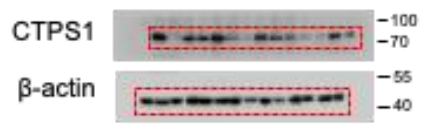

The loading control actin was run on the different gels

Supplementary Figure 2: Gating strategies of flow cytometry from Figures.

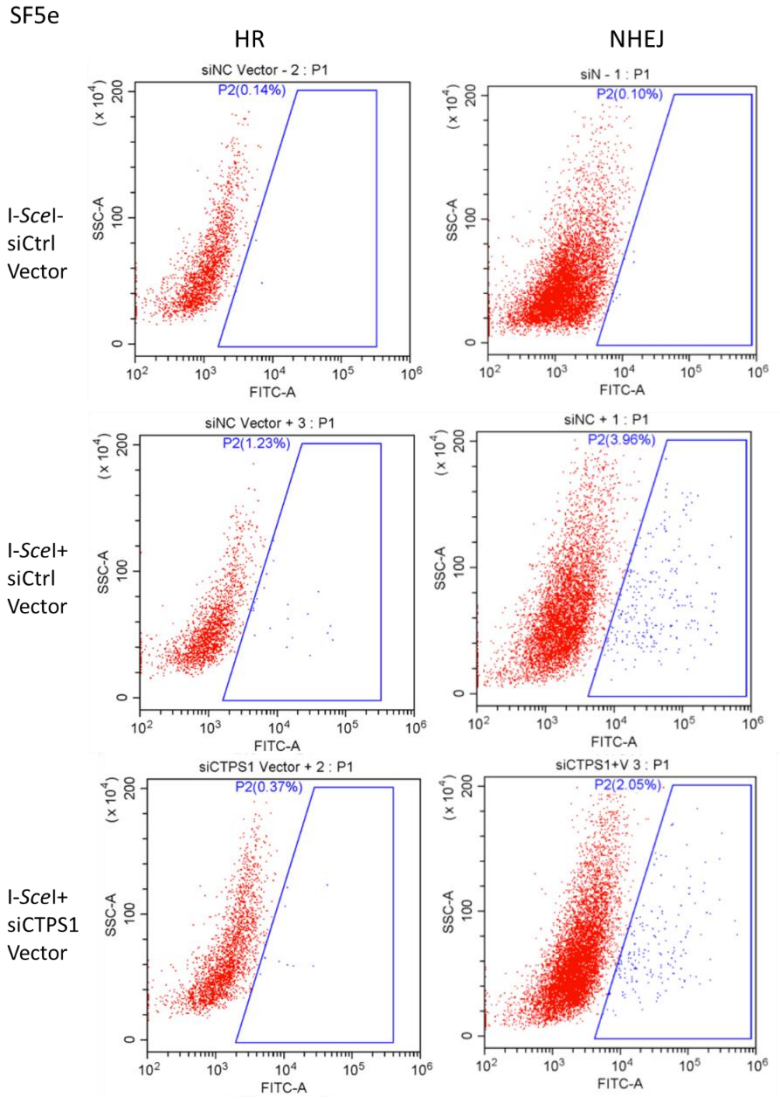

SF5e

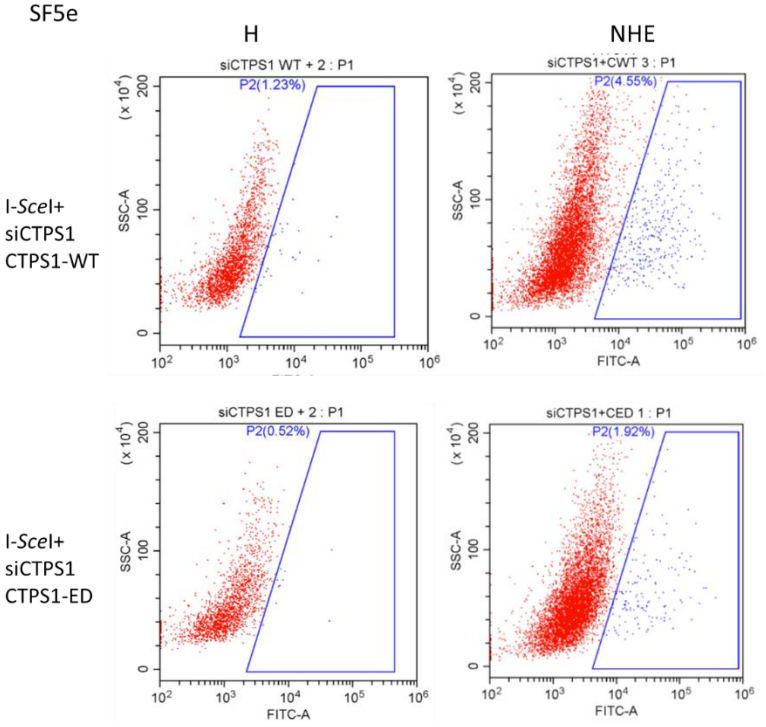
H
NHE
I-SceI+
siCTPS1
CTPS1-WT
siCTPS1 WT + 2 : P1
P2(1.23%)
siCTPS1+CWT 3 : P1
P2(4.55%)
I-SceI+
siCTPS1
CTPS1-ED
siCTPS1 ED + 2 : P1
P2(0.52%)
siCTPS1+CED 1 : P1
P2(1.92%)
SSC-A
FITC-A

SF5g

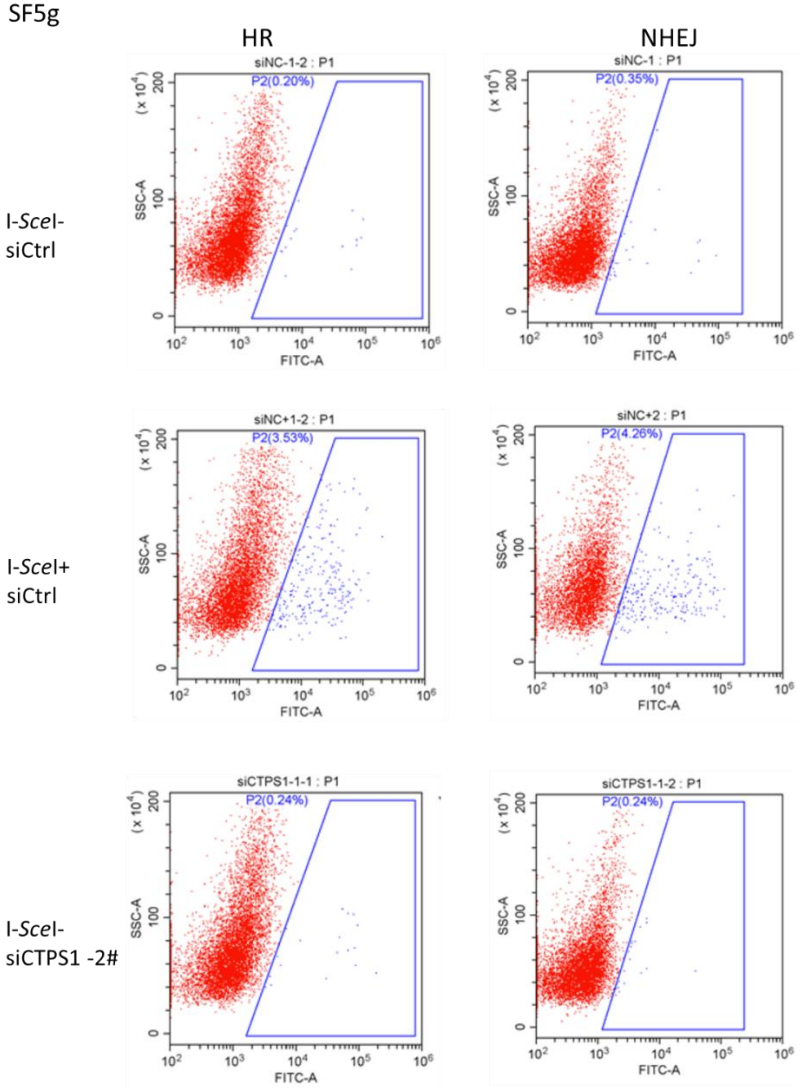
HR
NHEJ
I-SceI-siCtrl
I-SceI+siCtrl
I-SceI-siCTPS1 -2#
siNC-1-2 : P1
P2(0.20%)
siNC-1 : P1
P2(0.35%)
siNC+1-2 : P1
P2(3.53%)
siNC+2 : P1
P2(4.26%)
siCTPS1-1-1 : P1
P2(0.24%)
siCTPS1-1-2 : P1
P2(0.24%)
SSC-A
FITC-A

SF5g

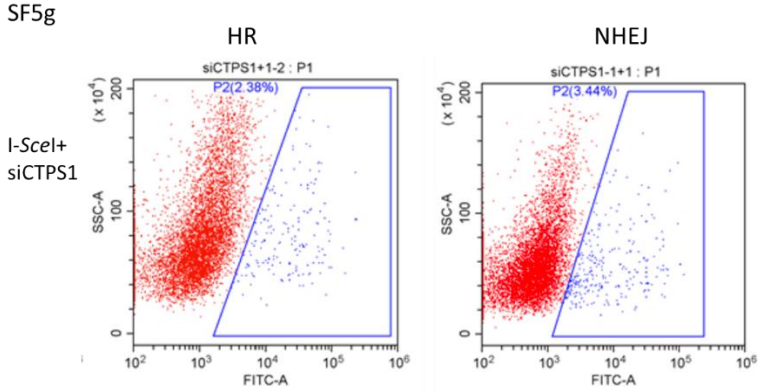
HR
NHEJ
I-SceI+siCTPS1
siCTPS1+1-2 : P1
P2(2.38%)
siCTPS1-1+1 : P1
P2(3.44%)
SSC-A
FITC-A

SF6d

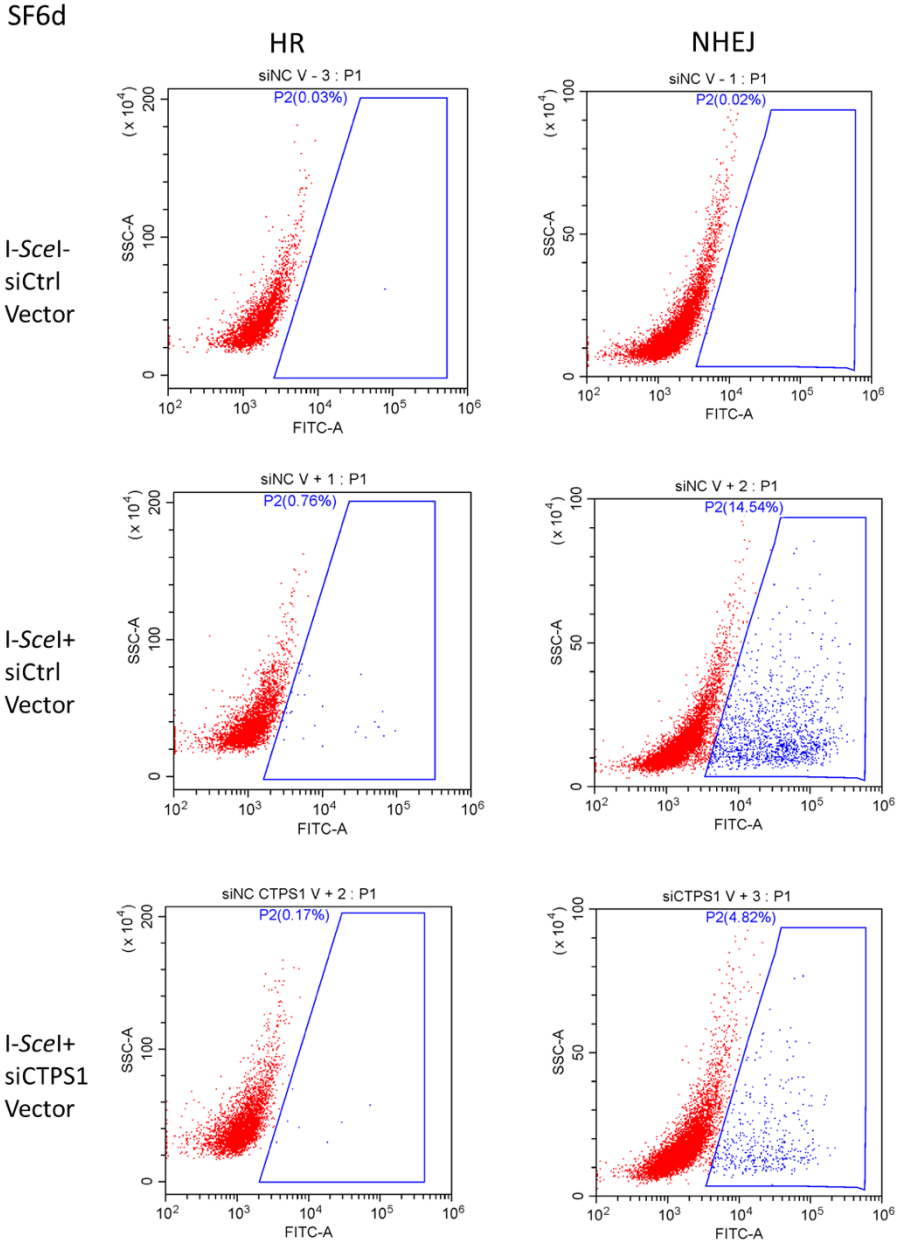
HR
NHEJ
I-SceI-
siCtrl
Vector
I-SceI+
siCtrl
Vector
I-SceI+
siCTPS1
Vector
siNC V - 3 : P1
P2(0.03%)
siNC V - 1 : P1
P2(0.02%)
siNC V + 1 : P1
P2(0.76%)
siNC V + 2 : P1
P2(14.54%)
siNC CTPS1 V + 2 : P1
P2(0.17%)
siCTPS1 V + 3 : P1
P2(4.82%)
SSC-A
FITC-A
(x 10^4)

SF6d

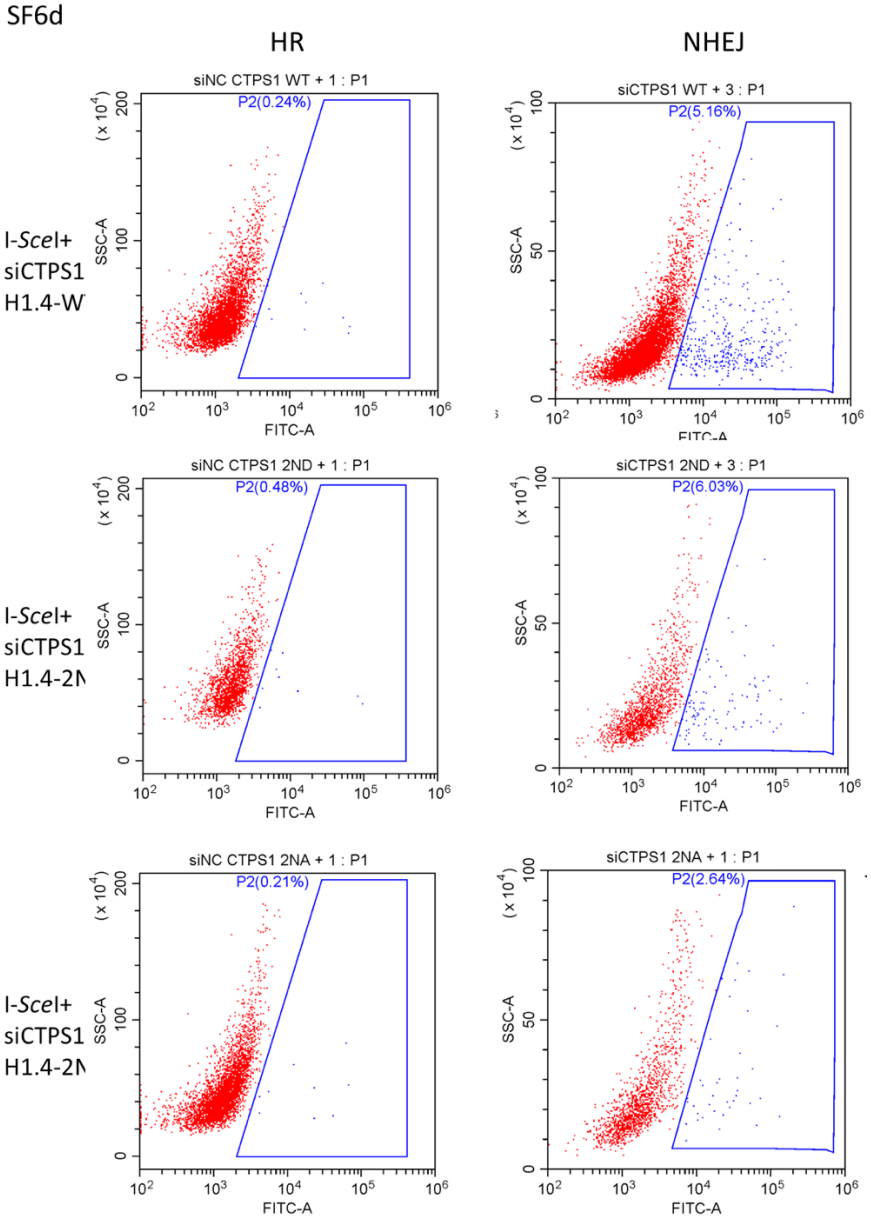
HR
NHEJ
I-SceI+ siCTPS1 H1.4-W
I-SceI+ siCTPS1 H1.4-2N
I-SceI+ siCTPS1 H1.4-2N
siNC CTPS1 WT + 1 : P1
P2(0.24%)
siCTPS1 WT + 3 : P1
P2(5.16%)
siNC CTPS1 2ND + 1 : P1
P2(0.48%)
siCTPS1 2ND + 3 : P1
P2(6.03%)
siNC CTPS1 2NA + 1 : P1
P2(0.21%)
siCTPS1 2NA + 1 : P1
P2(2.64%)
SSC-A
FITC-A

SF6d

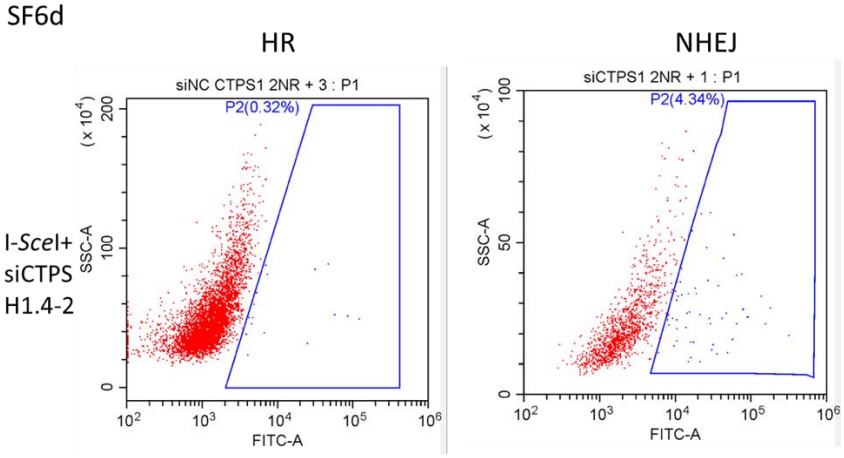
HR
NHEJ
I-SceI+ siCTPS H1.4-2
siNC CTPS1 2NR + 3 : P1
P2(0.32%)
siCTPS1 2NR + 1 : P1
P2(4.34%)
SSC-A
FITC-A

SF9e

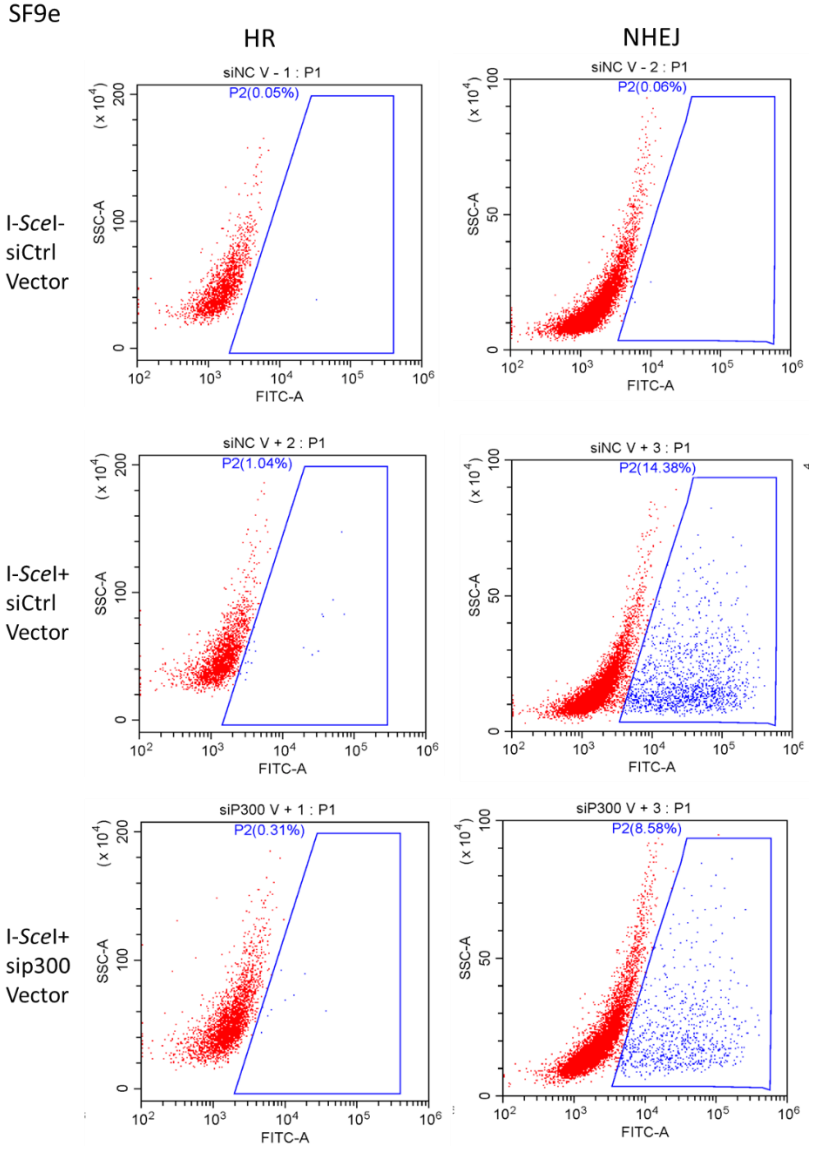
HR
NHEJ
I-SceI-
siCtrl
Vector
I-SceI+
siCtrl
Vector
I-SceI+
sip300
Vector
siNC V - 1 : P1
P2(0.05%)
siNC V - 2 : P1
P2(0.06%)
siNC V + 2 : P1
P2(1.04%)
siNC V + 3 : P1
P2(14.38%)
siP300 V + 1 : P1
P2(0.31%)
siP300 V + 3 : P1
P2(8.58%)
SSC-A
FITC-A
(x 10^4)

SF9e

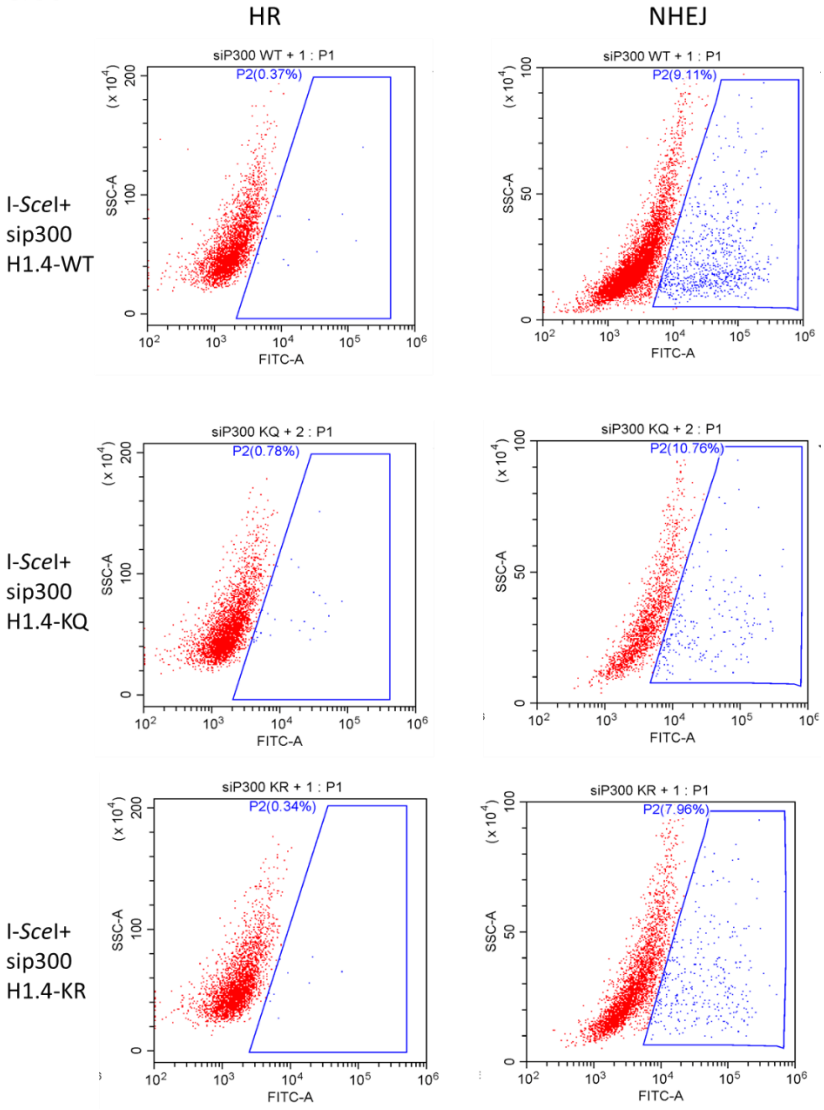
HR
NHEJ
I-SceI+ sip300 H1.4-WT
I-SceI+ sip300 H1.4-KQ
I-SceI+ sip300 H1.4-KR
siP300 WT + 1 : P1
P2(0.37%)
siP300 WT + 1 : P1
P2(9.11%)
siP300 KQ + 2 : P1
P2(0.78%)
siP300 KQ + 2 : P1
P2(10.76%)
siP300 KR + 1 : P1
P2(0.34%)
siP300 KR + 1 : P1
P2(7.96%)
SSC-A
FITC-A

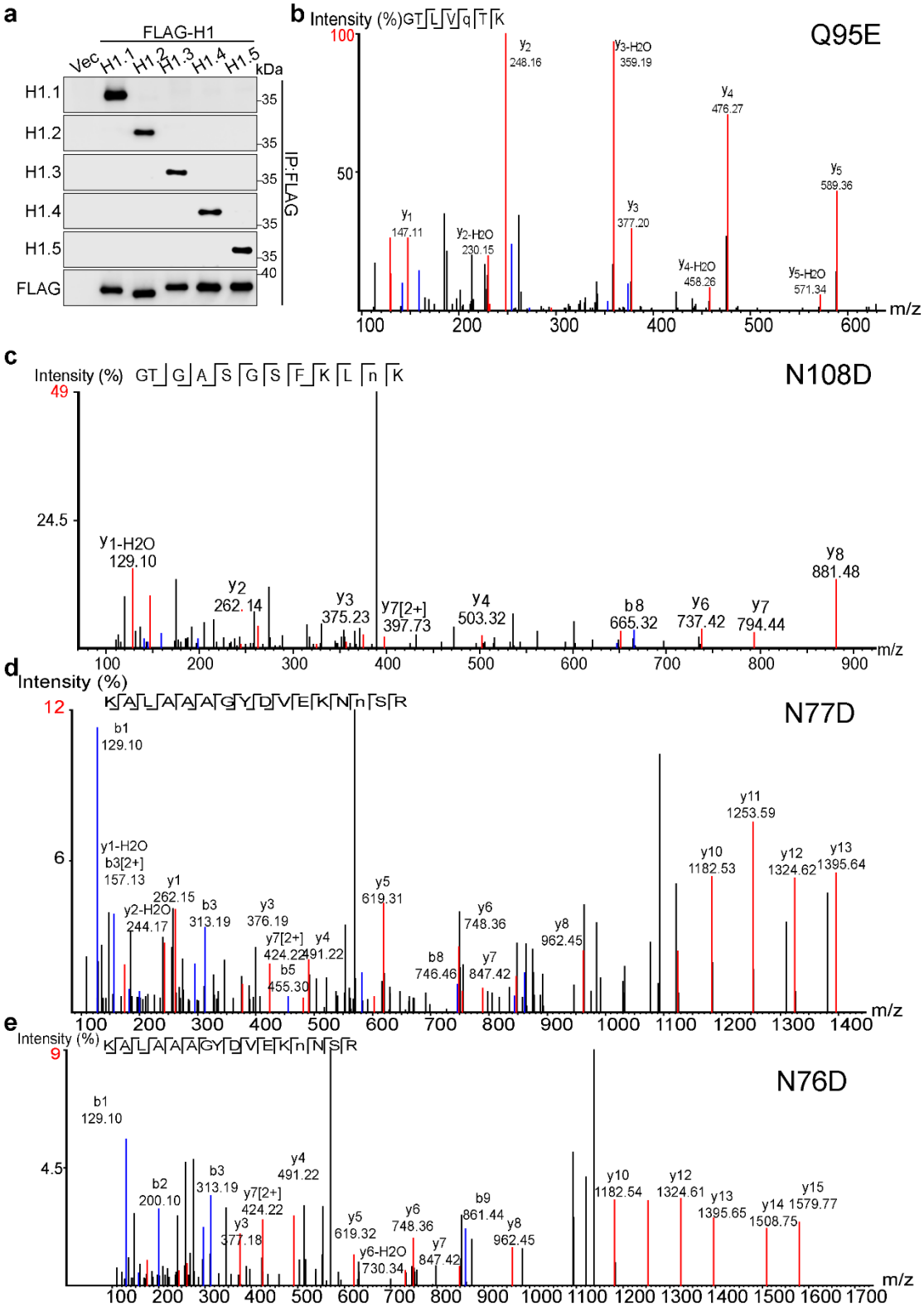

Supplementary Figure 3. DNA damage induces H1 Deamidation

(a) HeLa cells were transfected with indicated FLAG-H1 variant plasmids. WCLs were extracted, immunoprecipitated with anti-FLAG, and analyzed by western blotting.

(b-e) HeLa cells were exposed to 10 Gy IR and released for 2 min. Histones were

extracted and Q95 (b), N108 (c), N77 (d), and N76 (e) deamidated peptides were identified by MS.

Three independent experiments were performed in (a).

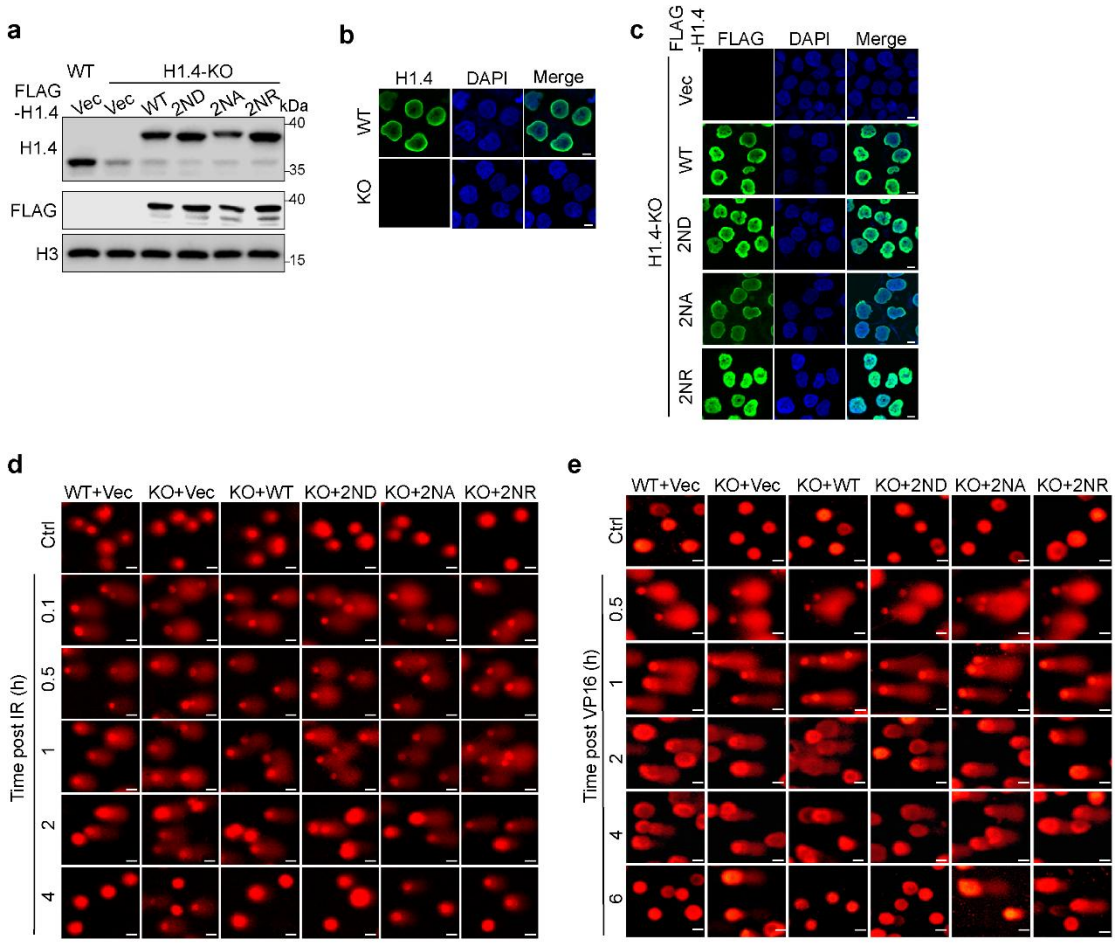
a
WT
H1.4-KO
FLAG -H1.4
Vec
Vec
WT
2ND
2NA
2NR
kDa
H1.4
40
35
FLAG
40
H3
15
b
H1.4
DAPI
Merge
WT
KO
c
FLAG -H1.4
FLAG
DAPI
Merge
H1.4-KO
Vec
WT
2ND
2NA
2NR
d
WT+Vec
KO+Vec
KO+WT
KO+2ND
KO+2NA
KO+2NR
Time post IR (h)
Ctrl
0.1
0.5
1
2
4
e
WT+Vec
KO+Vec
KO+WT
KO+2ND
KO+2NA
KO+2NR
Time post VP16 (h)
Ctrl
0.5
1
2
4
6

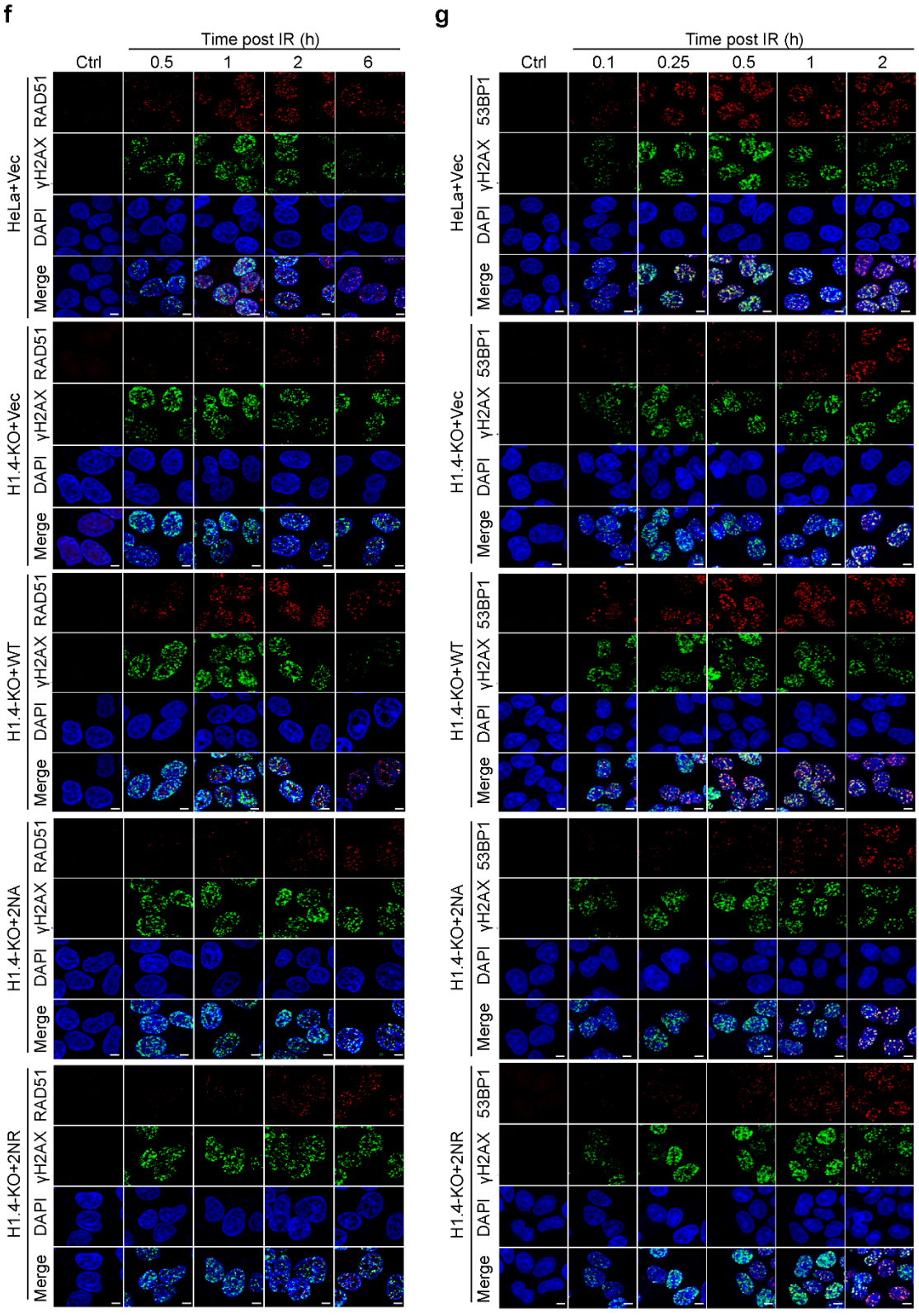

Supplementary Figure 4. Deamidation of H1 N76/77 is required for DNA damage repair

(a-c) WT or H1.4-KO HeLa cells with stable lentiviral introduction of WT or mutants FLAG-H1.4 were analyzed by western blotting (a), and immunofluorescence staining

using anti-H1.4 (b) or anti-FLAG (c). Immunofluorescence staining results confirmed that all cells with exogenous H1.4 expressed FLAG-tagged proteins, and western blotting results showed that the expression levels of endogenous and exogenous proteins were comparable. Scale bars, 5 μm.

(d and e) WT or H1.4-KO HeLa cell lines with stable expression of WT or mutants FLAG-H1.4 were exposed to IR (d) or VP16 (e) and analyzed by comet assay at the indicated times post-treatment. Representative images, taken from 50 cells per group, are shown. Scale bars, 10 μm.

(f and g) WT or H1.4-KO HeLa cell lines with stable expression of WT or mutants FLAG-H1.4 were exposed to 10 Gy IR and analyzed by immunofluorescence using anti-RAD51 and anti-γH2AX (f) or anti-53BP1 and anti-γH2AX (g) antibodies, at the indicated times post-treatment. Representative images, taken from 50 cells per group, are shown. Scale bars, 5 μm.

Three independent experiments were performed in (a–g).

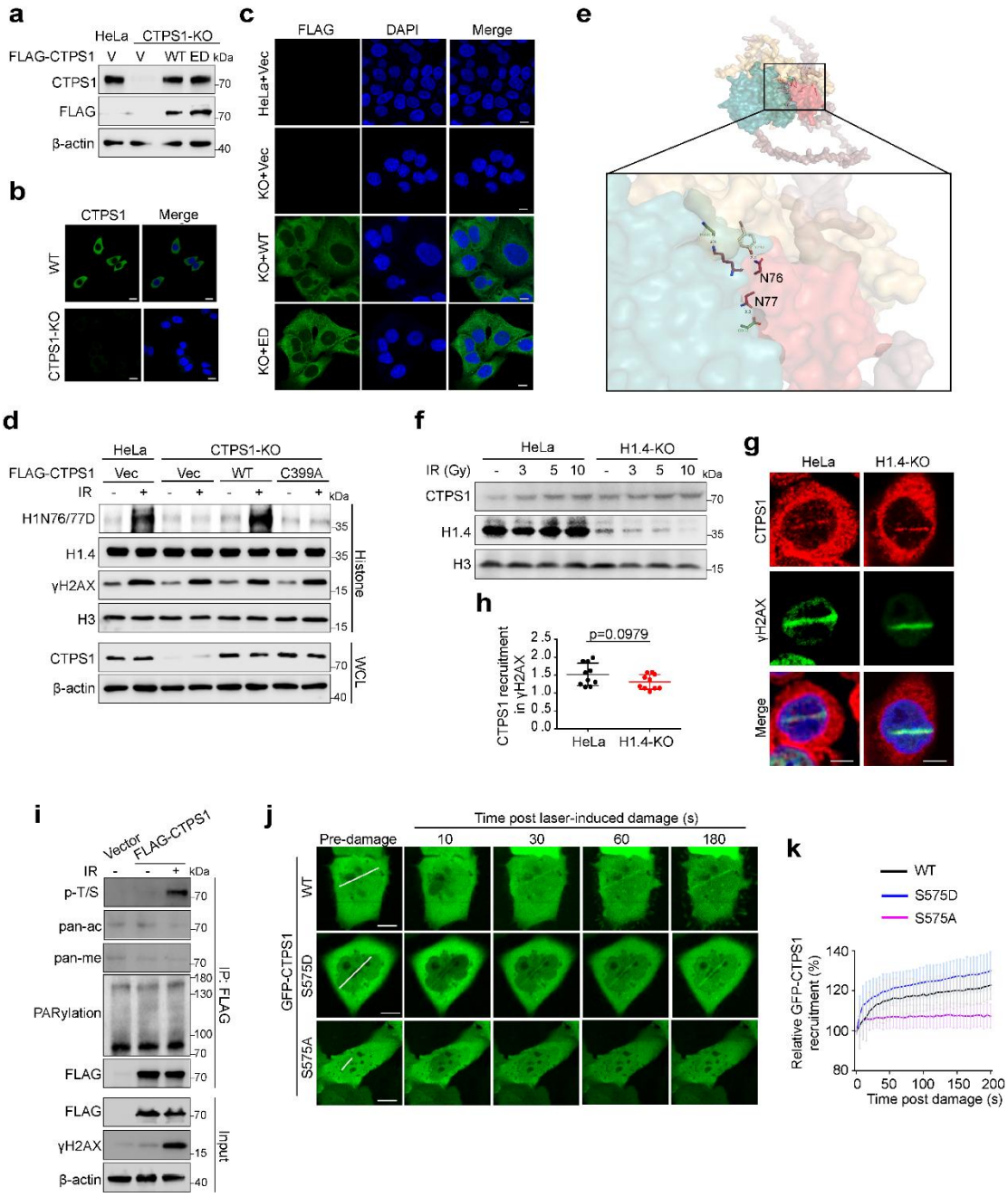

Supplementary Figure 5. CTPS1 deamidates H1 N76/77 in response to DNA damage

(a-c) WT or CTPS1-KO HeLa cells with stable integration of WT or CTPS1 mutant were analyzed by western blotting (a) and immunofluorescence staining using anti-CTPS1 (b) or anti-FLAG (c) antibodies. Immunofluorescence staining results confirmed that all cells with exogenous CTPS1 expressed FLAG-tagged proteins, and western blotting results showed that expression levels of endogenous and exogenous proteins were comparable. Scale bars, 5 μm.

(d) WT or CTPS1-KO HeLa cells expressing FLAG-CTPS1 WT or C399A were treated with or without 10 Gy IR. Histones and WCLs were analyzed by immunoblotting.

(e) Molecular-docking-predicted 3D structural image of the interaction between CTPS1 and H1.4 by GRAMM (gramm.compbio.ku.edu). Locations of the main interacting amino acids are shown; residues 76 and 77 are marked. Yellow, CTPS1; green, CTPS1-glutamine amidotransferase domain; red, H1.4 globular domain; brown, H1.4 C and N terminals.

(f) WT or H1.4-KO HeLa cells were exposed to indicated dose of IR. Chromatin was extracted for western blotting.

(g and h) WT or H1.4-KO HeLa cells were micro-irradiated, fixed at 5 min post-irradiation, and analyzed by immunofluorescence using anti-CTPS1 and anti-γH2AX antibodies. Representative images (g) and quantification of 10 cells (h) are shown. Scale bars, 5 μm.

(i) HeLa cells were transfected with FLAG-CTPS1 for 48 h and exposed or not to 10 Gy IR. WCLs were extracted, immunoprecipitated with anti-FLAG, and analyzed by western blotting.

(j and k) HeLa cells were transfected with GFP-tagged CTPS1-WT or CTPS1 mutant for 48 h and then micro-irradiated. Images were captured every 10 s for 5 min, and the irradiated path signal intensity in cells was calculated. Representative images (j) and quantification of 30 cells (k) are shown. Scale bars, 5 μm.

Data represent the means ± s.d. (h, k). n = 10 cells (h) or n = 30 cells (k) from three independent experiments. P values were calculated using Student unpaired two-tailed t-tests (h). Three independent experiments were performed in (a–d, f, h-k).

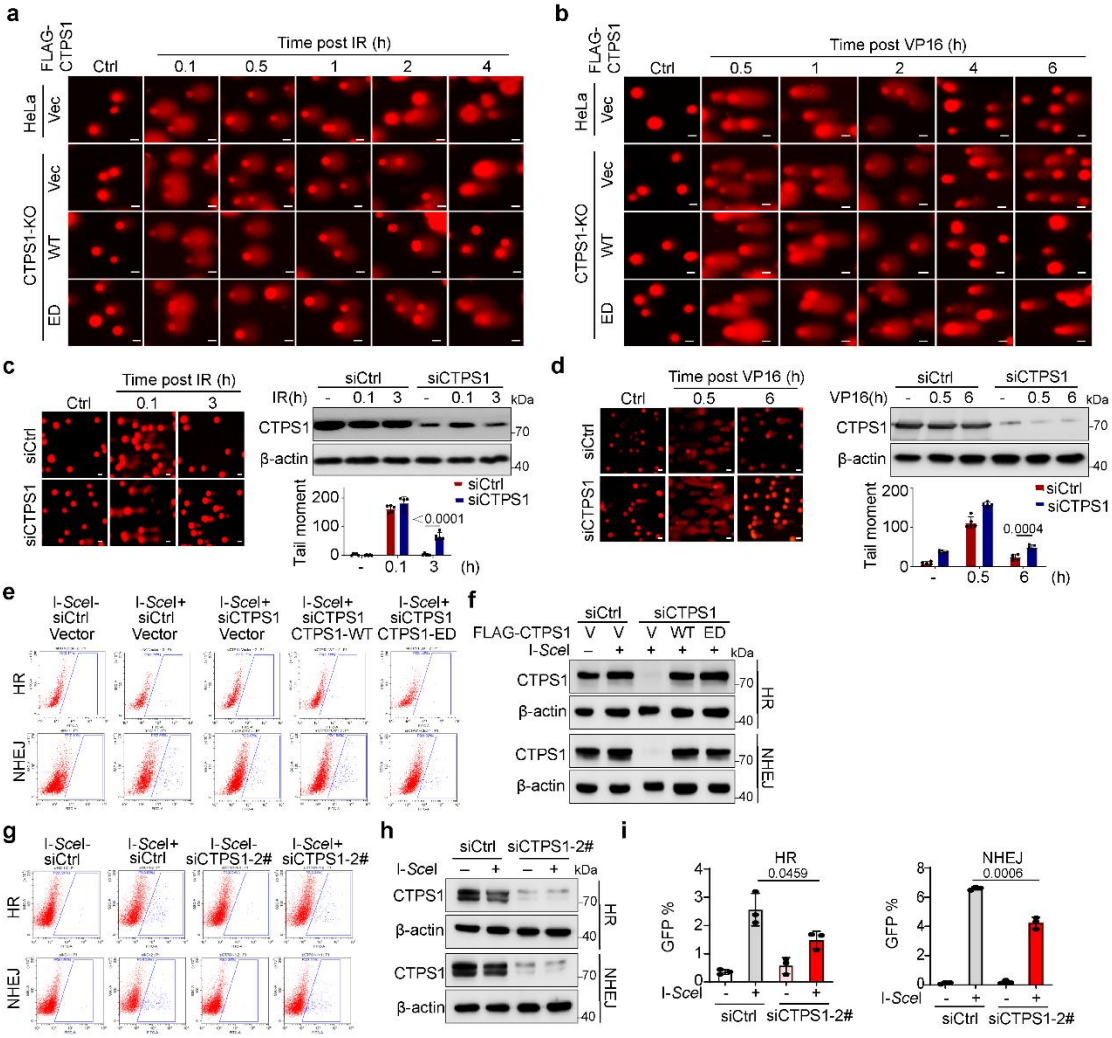
a
FLAG-CTPS1
Time post IR (h)
Ctrl
0.1
0.5
1
2
4
HeLa
Vec
CTPS1-KO
Vec
WT
ED
b
Time post VP16 (h)
Ctrl
0.5
1
2
4
6
c
Time post IR (h)
siCtrl
siCTPS1
IR(h)
kDa
CTPS1
β-actin
70
40
Tail moment
0.0001
(h)
d
Time post VP16 (h)
VP16(h)
0.0004
e
I-SceI- siCtrl Vector
I-SceI+ siCtrl Vector
I-SceI+ siCTPS1 Vector
I-SceI+ siCTPS1 CTPS1-WT
I-SceI+ siCTPS1 CTPS1-ED
HR
NHEJ
f
FLAG-CTPS1
V
WT
ED
I-SceI
g
I-SceI- siCtrl
I-SceI+ siCtrl
I-SceI- siCTPS1-2#
I-SceI+ siCTPS1-2#
h
i
GFP %
0.0459
0.0006

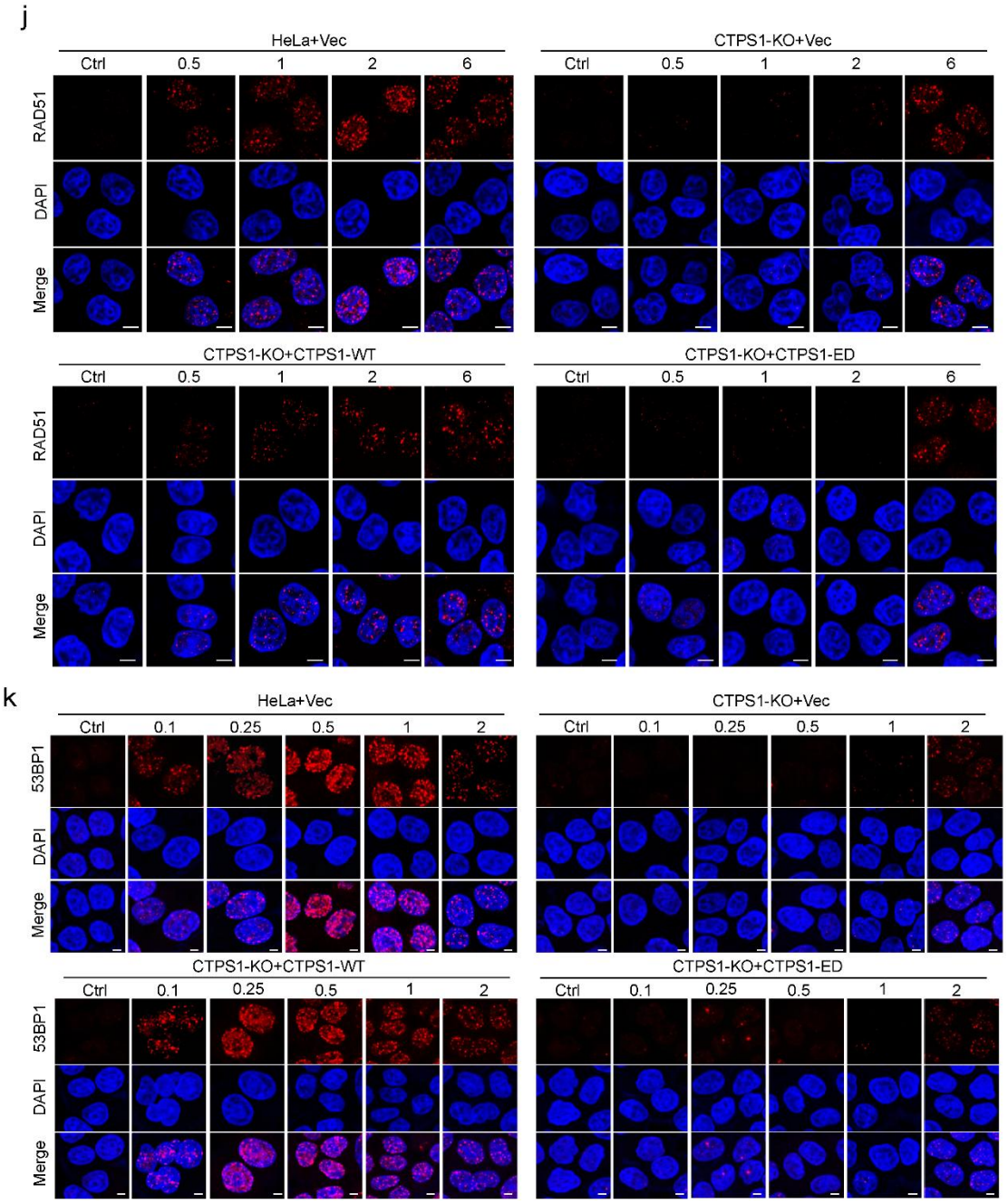

Supplementary Figure 6. CTPS1 deamidated-H1 N76/77 is required for DNA damage repair

(a-b) WT or CTPS1-KO HeLa cell lines stably expressing CTPS1-WT or CTPS1-ED were exposed to IR (a) and VP16 (b) and analyzed by comet assay at the indicated times post-treatment. Representative images of 50 cells in each group are shown. Scale bars, 10 μm.

(c and d) HeLa cells were transfected with the indicated siRNAs for 48 h, exposed to IR (c) or VP16 (d), and analyzed by comet assay at the indicated time post-IR or VP16

exposure. Representative images (left) and quantification of >50 cells from five fields in each group from three independent experiments (right-bottom) are shown. WCLs with the same treatment were extracted and analyzed by western blotting (right-top). Scale bars, 10 μm.

(e and f) pDR-GFP (e-top) or pEJ5-GFP (e-bottom) U2OS cells were transfected with the indicated siRNAs, followed by plasmids. Representative flow cytometry images of GFP expression (e) and western blots of WCLs (f) are shown.

(g and h) pDR-GFP (g-top) or pEJ5-GFP (g-bottom) U2OS cells were transfected with the indicated siRNAs. Representative flow cytometry images of GFP expression (g) and western blots of WCLs (h) are shown.

(i) Quantification of GFP expression for the experiments shown in (g).

(j-k) WT or CTPS1-KO HeLa cell lines stably expressing CTPS1-WT or CTPS1-ED exposed to 10 Gy IR and analyzed by immunofluorescence using anti-RAD51 (j) or anti-53BP1 (k) antibodies at the indicated times post-IR. Representative images, taken from 50 cells per group, are shown. Scale bars, 5 μm.

Data represent the means ± s.d. (c-d, i). n = 5 fields (c-d) or n = 3 samples (i) from three independent experiments. P values were calculated using Student unpaired two-tailed t-tests (c-d, i). Three independent experiments were performed in (a–k).

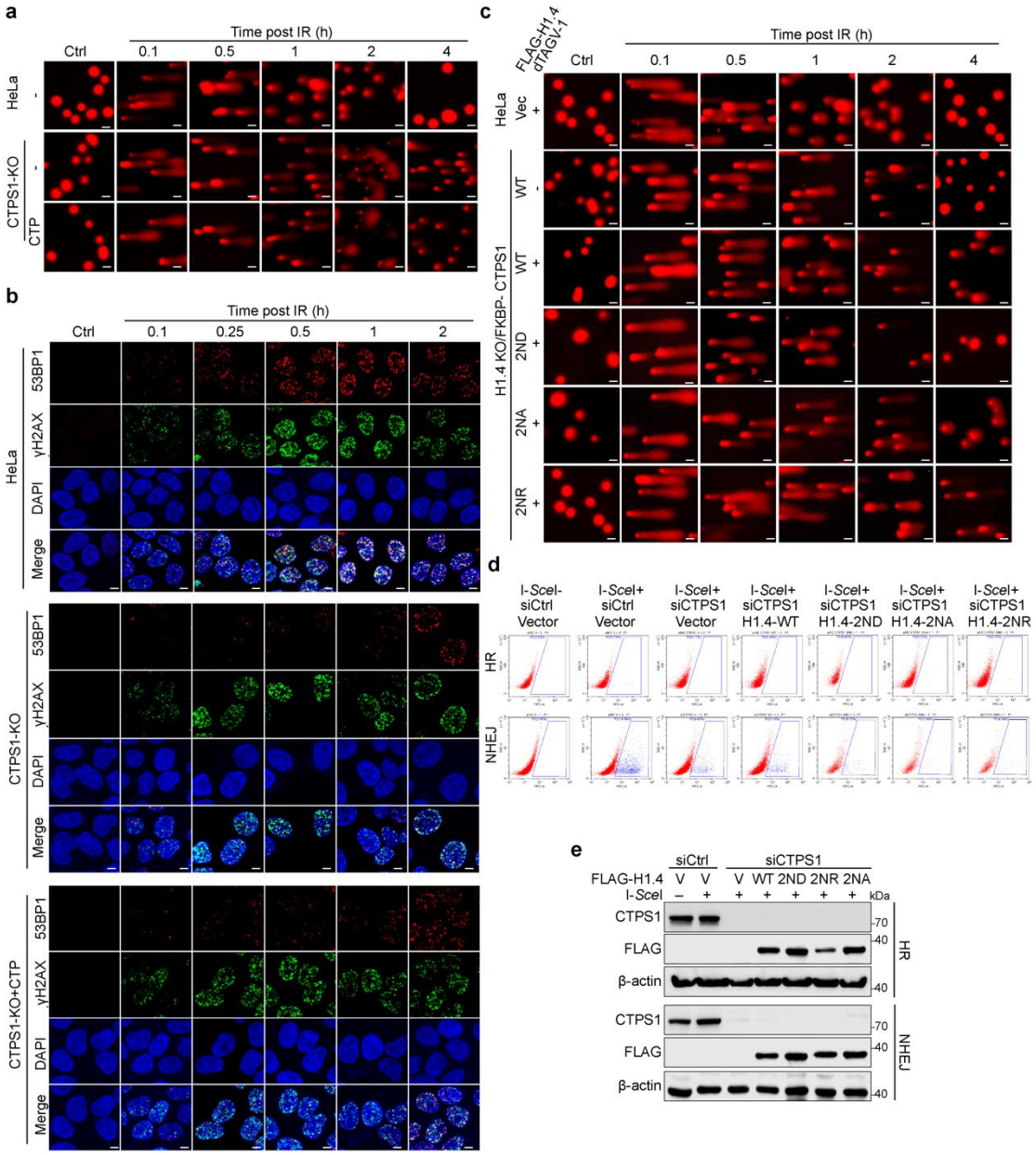
a
Time post IR (h)
Ctrl
0.1
0.5
1
2
4
HeLa
CTPS1-KO
CTP
b
Time post IR (h)
Ctrl
0.1
0.25
0.5
1
2
HeLa
CTPS1-KO
CTPS1-KO+CTP
53BP1
γH2AX
DAPI
Merge
c
FLAG-H1.4 dTAG V-1
Time post IR (h)
Ctrl
0.1
0.5
1
2
4
HeLa
Vec
H1.4 KO/FKBP-CTPS1
WT
2ND
2NA
2NR
d
I-SceI- siCtrl Vector
I-SceI+ siCtrl Vector
I-SceI+ siCTPS1 Vector
I-SceI+ siCTPS1 H1.4-WT
I-SceI+ siCTPS1 H1.4-2ND
I-SceI+ siCTPS1 H1.4-2NA
I-SceI+ siCTPS1 H1.4-2NR
HR
NHEJ
e
siCtrl
siCTPS1
FLAG-H1.4
V
WT
2ND
2NR
2NA
I-SceI
kDa
CTPS1
FLAG
β-actin
70
40
HR
NHEJ

f
Time post IR (h)
Ctrl
0.5
1
2
6
FKBP- CTPS1+H1.4-WT
FKBP- CTPS1+H1.4-WT+dTAGV-1
FKBP- CTPS1+H1.4-2ND+dTAGV-1
FKBP- CTPS1+H1.4-2NA+dTAGV-1
FKBP- CTPS1+H1.4-2NR+dTAGV-1
Merge
DAPI
γH2AX
RAD51
g
Time post IR (h)
Ctrl
0.1
0.25
0.5
1
2
FKBP- CTPS1+H1.4-WT
FKBP- CTPS1+H1.4-WT+dTAGV-1
FKBP- CTPS1+H1.4-2ND+dTAGV-1
FKBP- CTPS1+H1.4-2NA+dTAGV-1
FKBP- CTPS1+H1.4-2NR+dTAGV-1
Merge
DAPI
γH2AX
53BP1

Supplementary Figure 7. CTPS1 -mediated DNA damage repair is not dependent on CTP synthesis activity

(a) WT or CTPS1-KO HeLa cell lines were treated, or not, with 200 μM CTP for 2h, exposed to 10 Gy IR, and then analyzed by comet assay at the indicated times post-treatment. Representative images, taken from 50 cells per group, are shown. Scale bars, 10 μm.

(b) WT or CTPS1-KO HeLa cell lines were treated, or not, with 200 μM CTP for 2h, exposed to 10 Gy IR, and then analyzed by immunofluorescence for 53BP1 foci at the indicated times post-treatment. Representative images, taken from 50 cells per group, are shown. Scale bars, 5 μm.

(c) H1.4-KO HeLa cells stably expressing WT or mutant FLAG-H1.4 were modified to express FKBP-CTPS1, treated with dTAGV-1 for 3 h, and then exposed to IR. Cells were analyzed by comet assay at the indicated times post-IR. Representative images, taken from 50 cells per group, are shown. Scale bars, 10 μm.

(d and e) pDR-GFP or pEJ5-GFP U2OS cells were transfected with the indicated siRNAs and then plasmids. Representative flow cytometry images of GFP expression (d) and western blots of WCL (e) are shown.

(f and g) H1.4-KO HeLa cells stably expressing WT or mutant FLAG-H1.4 were modified to express FKBP-CTPS1, treated with dTAGV-1 for 3 h, and then exposed to IR. Cells were analyzed by immunofluorescence using anti-RAD51 and anti-γH2AX (f) or anti-53BP1 and anti-γH2AX (g) antibodies at the indicated times post-treatment. Representative images, taken from 50 cells per group, are shown. Scale bars, 5 μm.

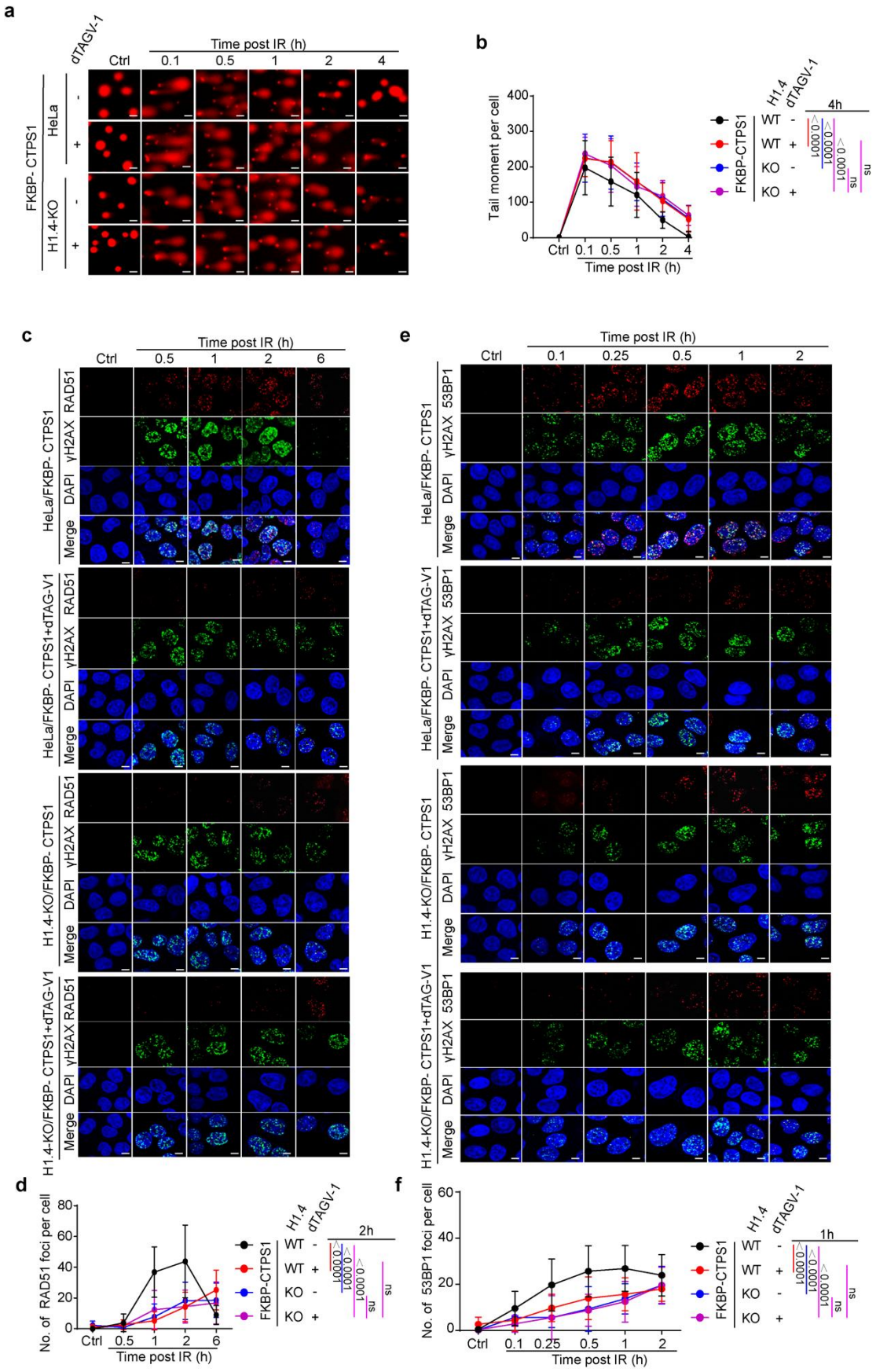

Supplementary Figure 8. CTPS1-H1.4 axis contributes to DNA damage repair

(a and b) WT or H1.4-KO HeLa cells were edited to express FKBP-CTPS1, treated or

not with dTAGV-1 for 3 h, and then exposed to IR (10 Gy). Cells were analyzed by comet assay at the indicated times post-treatment. Representative images (a) and quantifications (b) of 50 cells are shown. Statistical analyses of tail moment at 4 h post IR are shown. Scale bars, 10 μm.

(c-f) WT or H1.4-KO HeLa cells were edited to express FKBP-CTPS1, treated or not with dTAGV-1 for 3 h, and then exposed to IR (10 Gy). Cells were analyzed by immunofluorescence using anti-RAD51 and anti-γH2AX (c-d) or anti-53BP1 and anti-γH2AX (e-f) antibodies at the indicated times post-treatment. Statistical analyses of foci numbers at the 2 h (d) or 1 h (f) post IR are shown. Representative images (c and e) and quantifications (d and f) of 50 cells are shown. Scale bars, 5 μm.

Data represent the means ± s.d. (b, d, f). n = 50 cells (b, d, f) from three independent experiments. P values were calculated using Student unpaired two-tailed t-tests (b, d, f). Three independent experiments were performed in (a-f). The comet assay and foci formation of RAD51 and 53BP1 showed that both CTPS1 degradation and H1.4-KO cells exhibited defects in DNA repair efficiency. Furthermore, no additional effects were observed when both CTPS1 and H1.4 were simultaneously disrupted, confirming that the role of CTPS1 in DNA damage repair is primarily dependent on H1.

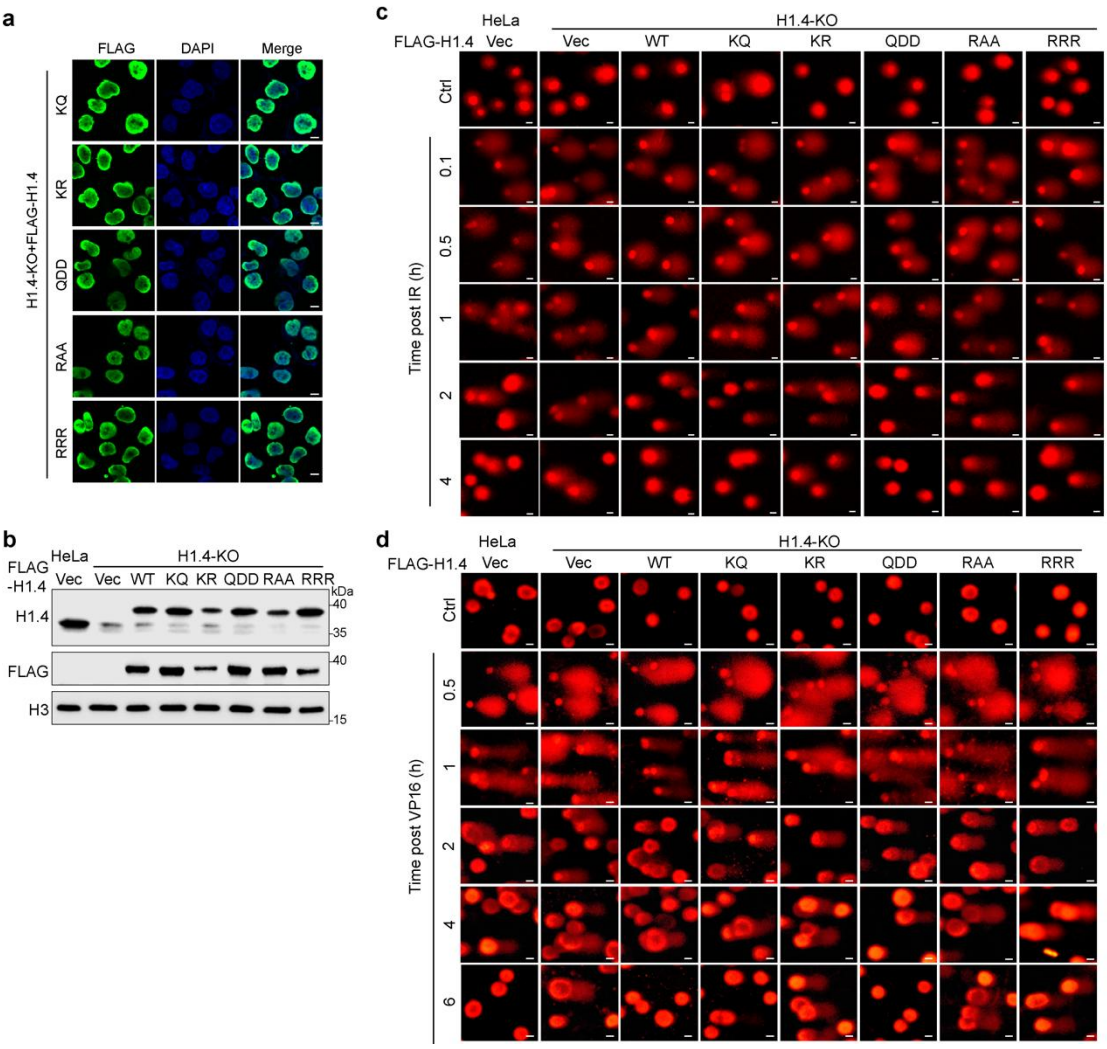
a
FLAG
DAPI
Merge
H1.4-KO+FLAG-H1.4
KQ
KR
QDD
RAA
RRR
b
HeLa
H1.4-KO
FLAG -H1.4
Vec
Vec
WT
KQ
KR
QDD
RAA
RRR
kDa
H1.4
40
35
FLAG
40
H3
15
c
HeLa
H1.4-KO
FLAG-H1.4
Vec
Vec
WT
KQ
KR
QDD
RAA
RRR
Ctrl
Time post IR (h)
0.1
0.5
1
2
4
d
HeLa
H1.4-KO
FLAG-H1.4
Vec
Vec
WT
KQ
KR
QDD
RAA
RRR
Ctrl
Time post VP16 (h)
0.5
1
2
4
6

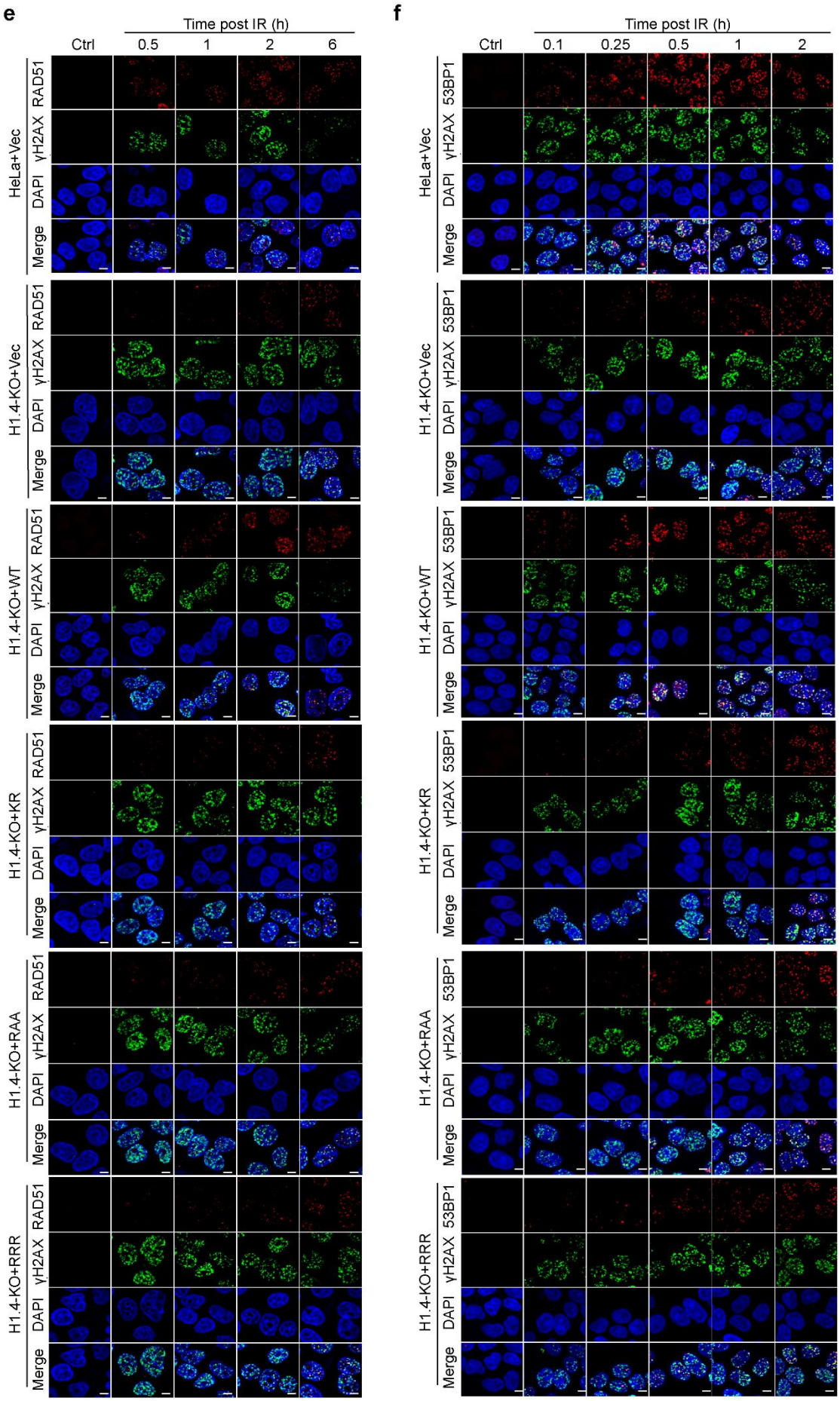
e
Time post IR (h)
Ctrl
0.5
1
2
6
HeLa+Vec
H1.4-KO+Vec
H1.4-KO+WT
H1.4-KO+KR
H1.4-KO+RAA
H1.4-KO+RRR
RAD51
γH2AX
DAPI
Merge
f
Time post IR (h)
Ctrl
0.1
0.25
0.5
1
2
53BP1
γH2AX
DAPI
Merge

Supplementary Figure 9. Deamidation of H1 N76/77 and acetylation of H1K75 is required for DNA damage repair

(a-b) H1.4-KO HeLa cells with stable lentiviral introduction of WT or mutants FLAG-H1.4 were analyzed by immunofluorescence (a) and western blotting (b) using anti-FLAG antibodies. Scale bars, 5 μm.

(c and d) WT or H1.4-KO HeLa cell lines with stable expression of WT or mutants FLAG-H1.4 were exposed to IR (c) or VP16 (d) and analyzed by comet assay at the indicated times post-treatment. Representative images, taken from 50 cells, per group are shown. Scale bars, 10 μm.

(e and f) WT or H1.4-KO HeLa cell lines with stable expression of WT or mutants FLAG-H1.4 were exposed to 10 Gy IR and analyzed by immunofluorescence using anti-RAD51 and anti-γH2AX (e) or anti-53BP1 and anti-γH2AX (f) antibodies at the indicated times post-treatment. Representative images, taken from 50 cells per group, are shown. Scale bars, 5 μm.

Three independent experiments were performed in (a–g).

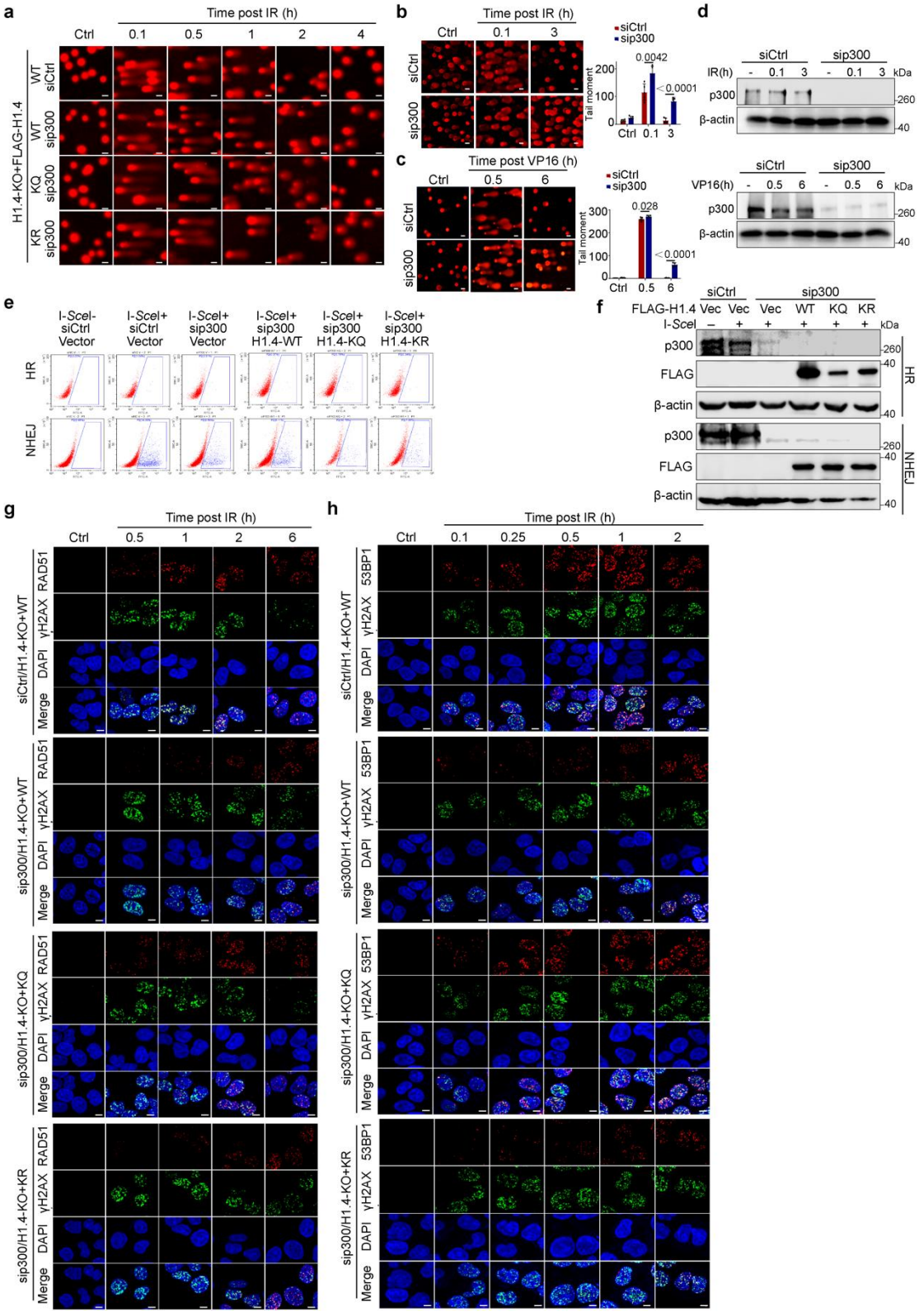

Supplementary Figure 10. p300 acetylated-H1K75 is required for DNA damage repair

(a) H1.4-KO HeLa cells stably expressing WT or mutant H1.4 were transfected with the indicated siRNAs, exposed to 10 Gy IR, and then analyzed by comet assay at the

indicated times post-IR. Representative images, taken from 50 cells per group, are shown. Scale bars, 10 μm.

(b and c) HeLa cells were transfected with the indicated siRNAs for 48 h, exposed to IR (b) or VP16 (c), and analyzed by comet assay at the indicated times after exposure. Representative images (left) and quantification of >50 cells from five fields per group (right) are shown. Scale bars, 10 μm.

(d) Cells were treated as in (b and c), and p300 was detected by western blotting.

(e and f) pDR-GFP or pEJ5-GFP U2OS cells were transfected with the indicated siRNAs followed by plasmids. Representative flow cytometry images of GFP expression (e) and western blots of WCLs using anti-p300 and anti-FLAG antibodies (f) are shown.

(g and h) H1.4-KO HeLa cells stably expressing WT or mutant H1.4 were transfected with the indicated siRNAs, exposed to 10 Gy IR, and analyzed by immunofluorescence using anti-RAD51 and anti-γH2AX (g) or anti-53BP1 and anti-γH2AX (h) antibodies at the indicated times post-treatment. Representative images, taken from 50 cells per group, are shown. Scale bars, 5 μm.

Data represent the means ± s.d. (b-c). n = 5 fields from three independent experiments (b-c). Three independent experiments were performed in (a-h).

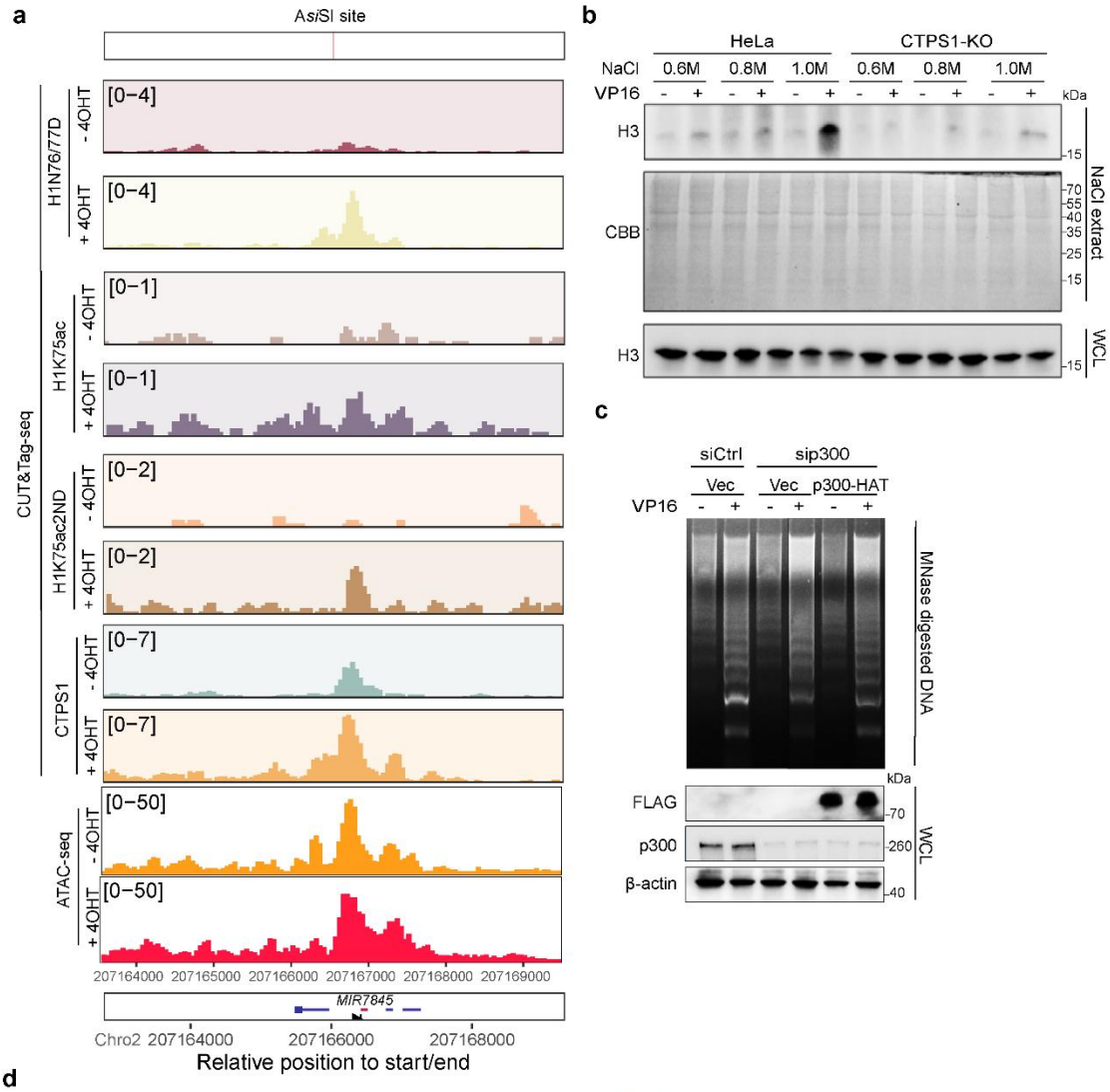
a
AsiSI site
CUT&Tag-seq
H1N76/77D
- 4OHT
+ 4OHT
[0–4]
[0–4]
H1K75ac
[0–1]
[0–1]
H1K75ac2ND
[0–2]
[0–2]
CTPS1
[0–7]
[0–7]
ATAC-seq
[0–50]
[0–50]
207164000 207165000 207166000 207167000 207168000 207169000
MIR7845
Chro2 207164000 207166000 207168000
Relative position to start/end
b
HeLa
CTPS1-KO
NaCl 0.6M 0.8M 1.0M 0.6M 0.8M 1.0M
VP16
kDa
H3
CBB
NaCl extract
H3
WCL
c
siCtrl
sip300
Vec
Vec p300-HAT
VP16
MNase digested DNA
kDa
FLAG
p300
β-actin
WCL
d
D77
Q75
D76
N77
K75
N76

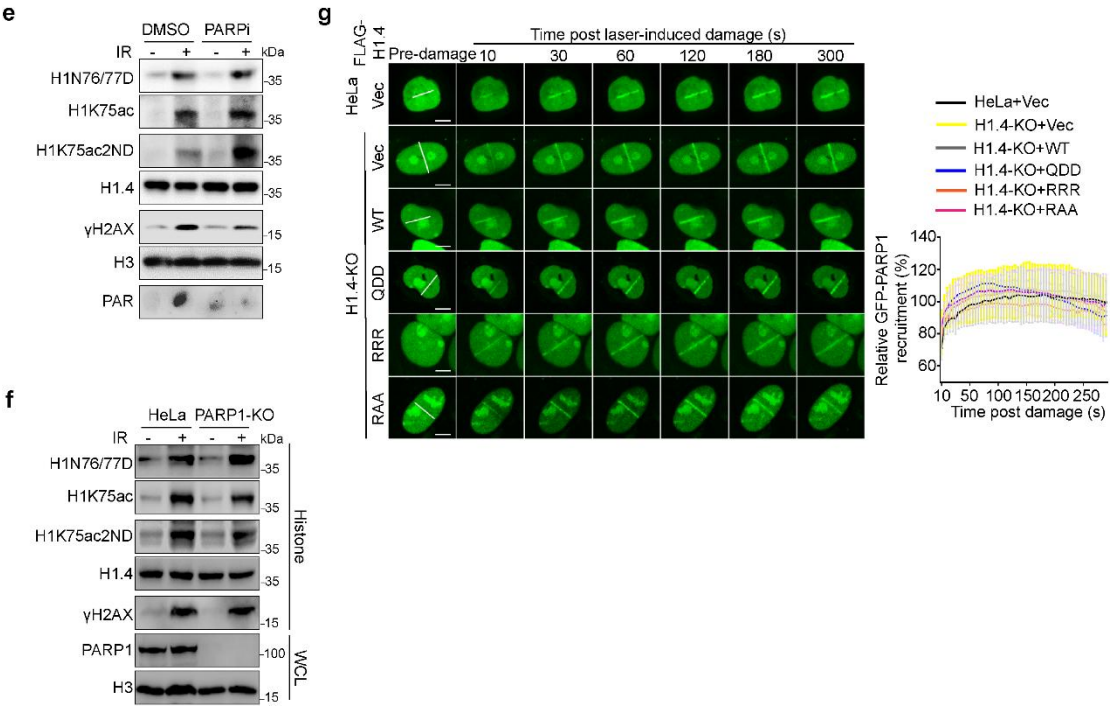

Supplementary Figure 11. Sequential H1N76/77 deamidation and H1K75 acetylation promotes chromatin relaxation

(a) U2OS-*Asi*SI-ER-AID cells were treated, or not, with 4OHT and subjected to ATAC-seq or CUT&Tag-seq with the indicated antibodies. A representative DSB site is shown.

(b) WT or CTPS1-KO HeLa cells were treated, or not, with VP16. Cell lysates were extracted using the indicated dose of NaCl buffer and analyzed by western blotting and CBB (top). WCLs were extracted and analyzed by western blotting (bottom).

(c) HeLa cells were transfected with the indicated siRNAs and plasmids for 48 h and treated, or not, with VP16. Chromatin fractions were extracted and analyzed by MNase sensitivity assay (top). WCLs were extracted and analyzed by western blotting (bottom).

(d) Locations of the main interacting amino acids between H1.4 and linker DNA are shown; residues 75, 76, and 77 are indicated. Blue, histone octamer; red, H1.4 globular domain.

(e) HeLa cells were treated with DMSO or PARP inhibitor (PARPi, Olaparib, 10 μM) for 4 h and then exposed to 10 Gy IR and released for 5 min. Histones were extracted for immunoblotting.

(f) WT or PARP1-KO HeLa cells were exposed to 10 Gy IR and released for 5 min. Histones or WCL were extracted for immunoblotting.

(g) WT or H1.4-KO HeLa cells with stable expression of mutant FLAG-H1.4 were transfected with GFP-PARP1 and then micro-irradiated. Images were captured every 10 s for 5 min, and the irradiated path signal intensity in five separate cells was calculated. Representative images (left) and quantification of five cells (right) are shown. Scale bars, 5 μm.

Data represent the means ± s.d. (g). n = 5 cells (g) from three independent experiments. Three independent experiments were performed in (b-c, e-g).

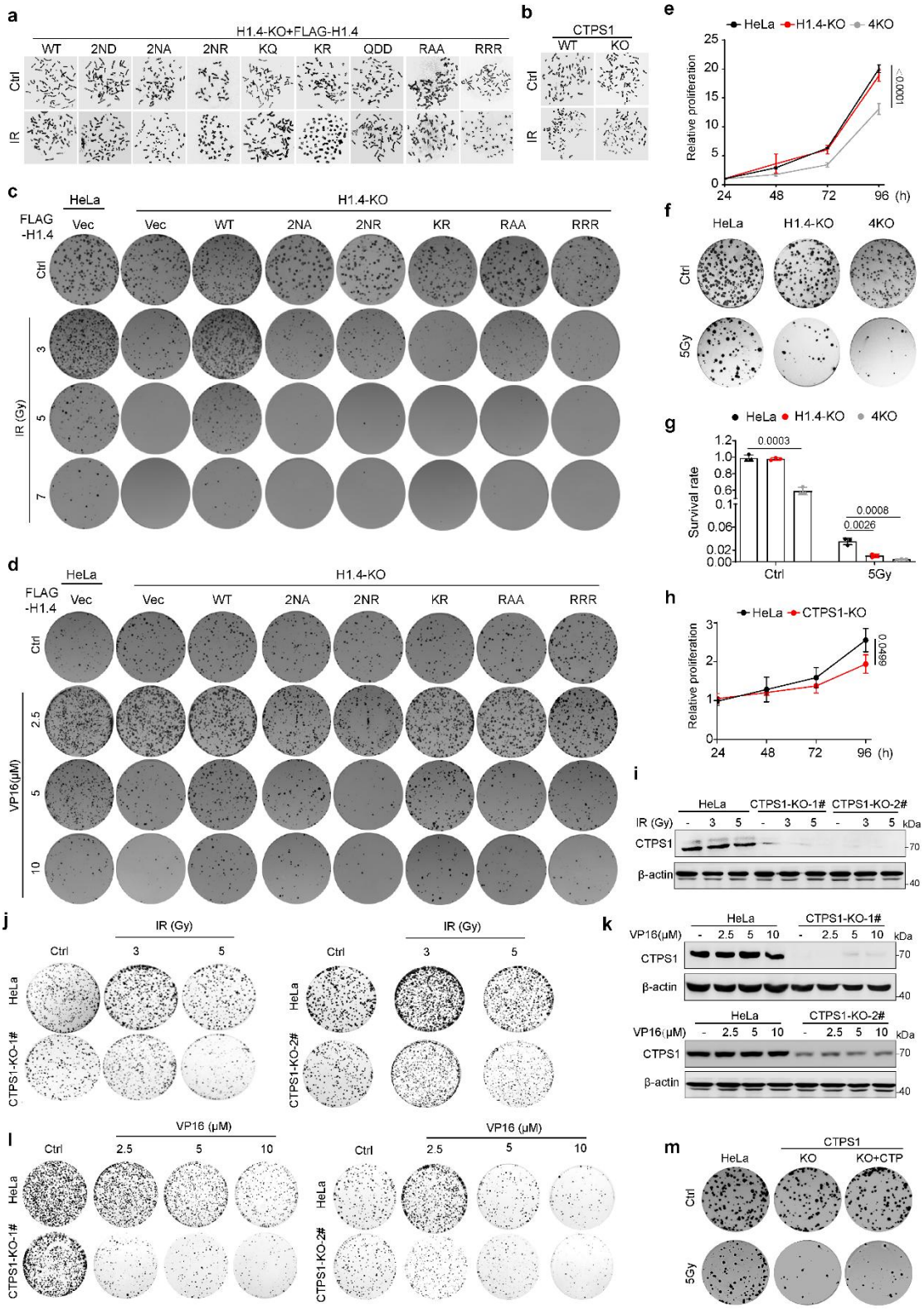

Supplementary Figure 12. Sequential H1N76/77 deamidation and H1K75 acetylation maintains genome stability

(a) H1.4-KO HeLa cells with stable expression of WT or H1.4 mutant were subjected to metaphase assay after IR exposure. Chromosomes were counterstained with Giemsa.

Representative images of chromosome aberrations, taken from >100 cells across five fields for each group, are shown.

(b) WT or CTPS1-KO HeLa cells were subjected to metaphase assay after IR exposure. Chromosomes were counterstained with Giemsa. Representative images of chromosome aberrations, taken from >100 cells across five fields for each group, are shown.

(c and d) WT or H1.4-KO HeLa cell lines with stable expression of WT or mutant H1.4 were subjected to colony formation assay after IR (c) or VP16 (d) treatment. Representative images are shown.

(e) WT, H1.4-KO, or 4KO HeLa cell lines were seeded in equal amounts and subjected to CCK-8 assay at the indicated time points after seeding. The absorbance of HeLa cells at 450 nm and recorded at 24 h, was normalized to 1. Statistical analyses at 96 h are shown.

(f and g) WT, H1.4-KO, or 4KO HeLa cell lines were subjected to colony formation assay after IR treatment. Representative images (f) and quantification of three independent experiments (g) are shown. The average colony numbers of HeLa cells without IR exposure were normalized to 1.

(h) WT and CTPS1-KO HeLa cell lines were seeded in equal amounts and subjected to CCK-8 assay at indicated time points after seeding. The absorbance of HeLa cells at 450 nm and recorded at 24 h, was normalized to 1. Statistical analyses at 96 h are shown.

(i-l) WT or CTPS1-KO HeLa cells were subjected to colony formation assay after IR (i-j) or VP16 (k-l) treatment. Representative images of three independent experiments are shown (j, l). WCLs after IR (i) and VP16 treatment (k) were analyzed by western blotting using CTPS1 antibodies.

(m) WT or CTPS1-KO HeLa cell lines were treated, or not, with 200 μM CTP for 2 h and exposed to IR. Cells were sub-seeded for colony formation assay. Representative images from three independent experiments are shown.

Data represent the means ± s.d. (e, g-h). n = 4 samples (e) or n=3 samples (g, h) from three independent experiments. P values were calculated using Student unpaired two-tailed t-tests (e, g, h). Three independent experiments were performed in (a-m).

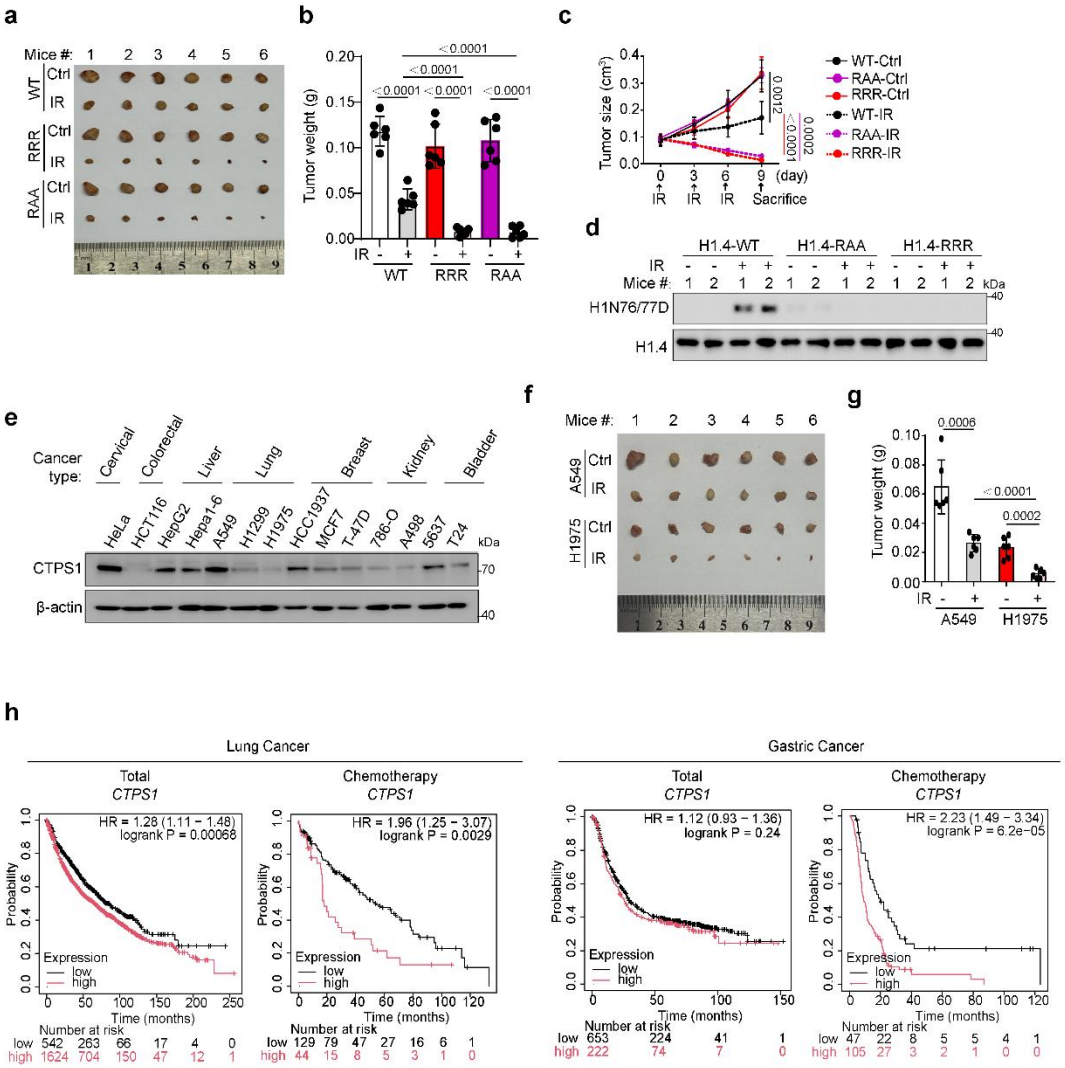

Supplementary Figure 13. CTPS1 is a potential therapeutic target for cancer

(a-d) H1.4-KO HeLa cells stably expressing WT-H1.4, RAA-H1.4, or RRR-H1.4 were injected into nude mice before treatment with or without IR (n = 6 per group). Tumor images (a), tumor weights (b), tumor growth curves (c) and western blot analysis of H1N76/77D and H1.4 in histone (d) from the xenograft mice are shown.

(e) WCLs were extracted from different cancer cell lines representing various tissues, and analyzed by western blotting.

(f and g) A549 or H1975 cells were injected into nude mice followed by treatment with or without IR (n = 6 per group). Tumor images (f) and tumor weights (g) from xenograft mice are shown.

(h) Overall survival curves of patients before exposure to chemotherapy relative to *CTPS1* expression in lung (left) and gastric (right) cancers.

Data represent the means ± s.d. (b-c, g). P values were calculated using Student unpaired two-tailed t-tests (b-c, g). Three independent experiments were performed in (e).

Supplementary Table 1. Primer sequences used in the experiments

Genes	Forward primer	Reverse primer
RT-PCR primers		
GMPS	CAGAGAGTCAAAGCCTGCAC	ACCCTGCACACCTACAGTTT
NADSYN1	AGGAGCAAGATACAGGCTTGG	GTCCGACTCGTAATAATGATCCC
PFAS	CCAGGGAAAGGAAGTCCGAT	GTGGTTGCACCACTAAAGGG
PPAT	CGAGAGGAATGTGGCGTGTT	CCCACGAGTCCCAGAGTGAT
CAD	TACGTGTCTCTCGCTCCTTC	CTGAGGCACCTTTACTCCCA
CTPS1	AGCTTGGCAGAAGCTCTGTA	CCAACTGCATCCCTAAGCAC
CTPS2	AACCGAGGACCCTGTGAAAT	TCACTGCTAGTTGCATCCCA
ASNS	TGCTGGCAGGATCAACTAGG	GTGTTGTGGTGCATGCCTAT
GFPT2	CTCATCGTGATTGGCTGTGG	GCAAACGTCATCCCTGAACA
ASNSD	GGGCGGGACTAAAGGAACTA	GAAGCAAACCAGACTGCACA
GFPT1	ACGGGAGACAGATTGTGGAG	ATCAGGCAGCCGTTTCAATC
ChIP qPCR primers		
Chr1-6 0.1 kb	GATTGGCTATGGGTGTGGAC	CATCCTTGCAAACCAGTCCT
Chr1-6 0.5 kb	CCTGGATATGAGTTTGATCAGC	CTCTCCTTTCGCTGACACTG
Chr1-6 1 kb	AGGAATTGACTGCGGTGTTC	GGGGAGGAGGAAAGGTGTAG
Chr1-6 2.5 kb	GCCATAACAGAGGGTGGAAA	AACTTTAGGATGGGGCTGCT
ChIP-re-ChIP qPCR primers		
Chr2-3 0.1 kb	CCATCAGGCATATCTTAGGACAG	AAACACGTGCGCAGCTGCAC
Chr2-3 0.5 kb	TATGTGGCTGGGACCCTAGGACA	GGGCCTCCTTTAACTGAACTAGT

Chr2-3 1 kb	TTCCCAAATGCCTTAAAAATCTGC	GCAATCTCTTTACTCGACCTTT
Chr2-3 5 kb	TAGAGAATGTGACACGGACAAGG	AATGTTAGAAAGAGGTGGCTTTA
Chr4-1 0.1 kb	CTTCCAGGATATCCCGCTGTTTGAT	GCGTGTTGCAAGAAATGCAAAAC
Chr4-1 0.5 kb	TGTAAGATGGTGCGATACAGTGT	TAAACGGAGGTGCCATTAAATAC
Chr4-1 1 kb	TGTGAGAAATCCTCATGGTAAAATG	GAGTTATGCTGCCTTGTGGAAT
Chr4-1 5 kb	AGCCACATGTGGCTGAAGCGG	CCTGGCTAATTTTTTTATATCACTT
Primers for plasmids construction		
H1.4 K75Q	ACGTGGAGCAAAACAACAGCCGCATCAAGC TGGGT	TGTTGTTTTGCTCCACGTCATAGCCAGCG GCTG
H1.4 K75R	ACGTGGAGCGAAACAACAGCCGCATCAAGC TGGGT	TGTTGTTTCGCTCCACGTCATAGCCAGCG GCTG
H1.4 N76/N77A	ACGTGGAGAAGgcagcaAGCCGCATCAAGC TGGGT	TtgctgcCTTCTCCACGTCATAGCCAGCG GCTG
H1.4 N76/N77R	ACGTGGAGAAGAGGAGGAGCCGCATCAAGC TGGGT	TCCTCCTTTCCTCCACGTCATAGCCAGCG GCTG
H1.4 N76/77D	ACGTGGAGAAGGACGACAGCCGCATCAAGC TGGGT	TGTCGTCCTTCTCCACGTCATAGCCAGCG GCTG
H1.4 RAA	TGGAGcgtgcagcaAGCCGCATCAAGCTGG GT	GCTtgctgcacgCTCCACGTCATAGCCAG CGG
H1.4 RRR	ACGTGGAGAGGAGGAGGAGCCGCATCAAGC TGGGT	TCCTCCTCCTCTCCACGTCATAGCCAGCG GCTG
H1.4 QDD	ACGTGGAGCAAGACGACAGCCGCATCAAGC TGGGT	TGTCGTCTTGCTCCACGTCATAGCCAGCG GCTG
FLAG-H1.4	caagcttgcggccgcgaattcaATGTCCGA GACTGCGCCTG	cagggatgccacccgggatccCTACTTTT TCTTGGCTGCCGC
GST-H1.4	gatctggttccgcgtggatccATGTCCGAG ACTGCGCCTG	gtcacgatgcggccgctcgagCTACTTTT TCTTGGCTGCCGC
HIS-H1.4	cagcaaatgggtcgcggatccATGTCCGAG ACTGCGCCTG	ttgtcgacggagctcgaattcCTACTTTT TCTTGGCTGCCGC
H1.4 sgRNA-1 mutation	gagactgcgcctgccgcgcccgctgctccg gcccctGCTGAGAAAACTCCAGTGAAA	gcgcttggccgcacctgcagacttgcggg ccttcttTTTCACTGGAGTTTTCTCAGC
H1.4 sgRNA-2 mutation	tgccaaacgcaaggcgtcgGGGCCCCCGGT GTCCGAG	acgccttgcgtttggcagcACCTGCAGAC TTGCGGGC
Lenti-FLAG-H1.4	gattctagagctagcgaattcATGGACTAC AAAGACCATGACGGTGATTAT	gatccatttaaattcgaattcCTACTTTT TCTTGGCTGCCGC
FLAG-H1.1	aaggatgacgatgacaagcttatgtctgaa acagtgcctcc	cagggatgccacccgggatccttacttttt tcttgggtgccg

FLAG-H1.2	aaggatgacgatgacaagcttatgtccgagactgctcctgc	cagggatgccacccgggatccctatttcttcttgggcgccg
FLAG-H1.3	aaggatgacgatgacaagcttatgtcggagactgctccact	cagggatgccacccgggatcctcacttttcttcggagctg
FLAG-H1.5	aaggatgacgatgacaagcttatgtcggaaaccgctcctgc	cagggatgccacccgggatccctacttcttttggcagccg
CTPS1 C399A	TTTTGGGCGTGgccTTAGGGATGCAGTTGGCAGTG	TAAggcCACGCCCAAAAAAGGCTTTTTCTGAT
CTPS1 H526/E528A	AGTACgcccctgcgTTCCTGTCCAGGCCTATCAAGC	GAAcgcaggggcGTACTGAACCCCAACAAAAAAGGG
CTPS1 S595A	gccCCTGACTCTGAAATCACCGAACTGAAGTT	ATTTCAGAGTCAGGggcGCTGCTTCCACTCCTGTCACTAT
CTPS1 S595D	CgacCCTGACTCTGAAATCACCGAACTGAAGT	TTTCAGAGTCAGGgtcGCTGCTTCCACTCCTGTCACTAT
HIS-CTPS1	cagcaaatgggtcgcggatccATGAAGTACATTCTGGTTACTGGTGG	ttgtcgacggagctcgaattcTCAGTCATGATTTATTGATGGAAACTT
CTPS1-EGFP	agcccgggcggatccaagcttATGAAGTACATTCTGGTTACTGGTGG	gctcaccattctagactcgagGTCATGATTTATTGATGGAAACTTCAG
CTPS1 sgRNA mutation	gacgttagcagcatatatCGAGTCCCCTTGTTGTTAGAGG	atatatgctgctaacgtcGTGGACACAGATCACTTGTTCAGG
Lenti-CTPS1-FLAG	gattctagagctagcgaattcATGAAGTACATTCTGGTTACTGGTGG	gatccatttaaattcgaattcCTACTTGTCATCGTCATCCTTGTAATCG
P300 D1399A	TTACCTCgctAGTGTTCATTTCTTCCGTCCTAAAT	GAACACTagcGAGGTAAGATATGTATACTCTCCTCTGGTT
GST-P300 D1	ttccaggggcccctgggatccATGGCCGAGAATGTGGTGG	ctcgagtcgacccgggaattcCTAATCCGGCGTAGGAAATATGG
GST-P300 D2	ttccaggggcccctgggatccGATCCTGCTGCTTTAAAAGACAGA	ctcgagtcgacccgggaattcCTAAGTAGATGGAGGATTTGATACCTGT
GST-P300 D3	ttccaggggcccctgggatccAATTCTCAGGCCATTGCTGAGA	ctcgagtcgacccgggaattcCTAGTAACTGTAATAAGTGGCATCACGA
GST-P300 D4	ttccaggggcccctgggatccACATCACGGGTATACAAATACTGCTC	ctcgagtcgacccgggaattcCTAGCATTCATTGCAGGTGTAGACA
GST-P300 D5	ttccaggggcccctgggatccCCCTGCGATCTGATGGATGG	ctcgagtcgacccgggaattcCTATTGAGTCCTGGGCAAGTAGG
GST-P300 D6	ttccaggggcccctgggatccCCACCCCTTCCAGGGCCC	ctcgagtcgacccgggaattcCTAGTGTATGTCTAGTGTACTCTGTGAGAGG
GST-P300 HAT	ttccaggggcccctgggatccATTGTGAAGAGCCCCATGGA	ctcgagtcgacccgggaattcCTACAGGCGGCGAGAATCG
FLAG-P300 HAT	aaggatgacgatgacaagcttATGATTGTGAAGAGCCCCATGG	cagggatgccacccgggatccCTACAGGCGGCGAGAATCG
P300 HAT-EGFP	cgctctagcccgggcggatccATGATTGTGAAGAGCCCCATGG	tctgtcgacgatatcgaattcCAGGCGGCGAGAATCGCC
P300 HAT-mCherry	tcgagctcaagcttcgaattcATGATTGTGAAGAGCCCCATGG	atggtggcgaccggtggatccaCAGGCGGCGAGAATCGCC

FKBP-CTPS1-H1	caggtcgactctagaggatccgcatcgtacgcgtacgtgtttggtagagatgcggtttcccatatt	gagacaaaggcttggccataatgtacttcattttactctttgacctggaagaagga
FKBP-CTPS1-BSD	tatggccaagcctttgtctca	tctttgtagtcaggtccagggttctcctcca
FKBP-CTPS1-FKBP	cctggacctgactacaaagaccatgacggtgatt	tttcatagaaccacctccgccttcc
FKBP-CTPS1-H2	gcggaggtggttctatgaaatatatcctggttactggtggtgttatatcag	aaaacgacggccagtgaattcgcatcgtacgcgtacgtgtttggctcaacgctagagagtaggagtacg

Supplementary Table 2. siRNA sequences used in the experiments

Target	siRNA
Ctr siRNA	UUCUCCGAACGUGUCACGUTT
CTPS1-1#	GCAGGAACAUUCUCUCCUUTT
CTPS1-2#	CCUAUGCCUCUGUCAUUAATT
P300	GGACUACCCUAUCAAGUAAUU
Tip60	GACGUAAGAACAAGAGUUAUU
CBP	GGCCUCCUCAAUAGUAACUTT
PCAF	UCGCCGUGAAGAAAGCGCATT
hMOF	GUGAUCCAGUCUCGAGUGATT
GMPS	GGGAAAGUCAUAGACCGAATT
NADSYN1	GGAUUUACUUGCUGGCCAATT
PFAS	GCCGGCUAUUGCUUUGGAATT
PPAT	GAAUGGGUCUUGUAAAUCATT
CAD	GCUAGUGCGUGCAGCCUUUTT
CTPS2	GGAUGCAACUAGCAGUGAUTT
ASNS	CCAAAUGGCAAAGUUGCAUTT
GFPT2	GCUUCUGAUGCAAGCGCUATT
ASNSD	GGCAUUUGUUGUUCUGUAATT
GFPT1	GGAGAGAGUUAUCCAACAATT
H1.1	AUAAAGUGGUAUAAACCUGAC

H1.2	GAAGCCAAGCCCAAGGUUATT
H1.3	UAAGUAAUCUCAAACUGUCAG
H1.4	CGGCGAAGAAGCCCAAGAATT
H1.5	AUCUAAAGAGCAGGUUUUGCG

Supplementary Table 3. sgRNA sequences used in the experiments

Target	sgRNA
CTPS1	GGTAGATGGATGAGACATCG
H1.4-1	GCCGAGAAGACTCCCGTGAAG
H1.4-2	GCGGCCAAGCGCAAAGCGTCT
H1.1	CAGGAGCAGCAGAAGCGGCG
H1.2	GGTACGCCTCGTAAGGCGTC
H1.3	CGCAAGCGCTTTCTTAAGCG
FKBP-CTPS1	GAGTAAAATGAAGTACATTC

Supplementary Table 4. Antibodies used in the experiments

RESOURCE	SOURCE	IDENTIFIER	Dilution
Rabbit monoclonal anti-H1.1 [66]	Abcam	Cat# ab254394	1:1000
Rabbit polyclonal anti-H1.2 [67]	Abcam	Cat# ab4086 RRID:AB_2117983	1:1000
Rabbit monoclonal anti-H1.3 [68]	Abcam	Cat# ab183736	1:1000
Rabbit polyclonal anti-H1.4 [69]	Cell Signaling Technology	Cat# 41328S RRID:AB_2799199	1:1000
Rabbit polyclonal anti-H1.5 [70]	Abcam	Cat# ab18208 RRID:AB_470263	1:1000
Rabbit polyclonal anti-H3 [71]	Proteintech	Cat# 17168-1-AP RRID:AB_2716755	1:1000
Mouse monoclonal anti-γH2AX [72]	Cell Signaling Technology	Cat# 80312 RRID:AB_2799949	1:1000
Mouse monoclonal anti-β-actin [73]	Proteintech	Cat# 66009-1-Ig RRID:AB_2687938	1:1000
Mouse monoclonal anti-FLAG® M2 [74]	Sigma-Aldrich	Cat# F3165 RRID:AB_259529	1:1000
Rabbit monoclonal anti-pATR [75]	Cell Signaling Technology	Cat# 30632 RRID:AB_2798992	1:1000
Rabbit polyclonal anti-pNF-κB [76]	Cell Signaling Technology	Cat# 3037 RRID:AB_2341216	1:1000
Rabbit polyclonal anti-53BP1 [77]	Novus Biologicals	Cat# NB100-304 RRID:AB_10003037	1:1000
Rabbit monoclonal anti-RAD51 [78]	Abcam	Cat# ab133534 RRID:AB_2722613	1:1000
Rabbit polyclonal anti-CTPS1 [79]	Proteintech	Cat# 15914-1-AP RRID:AB_2086513	1:1000
Rabbit polyclonal anti-GST [80]	Proteintech	Cat# 10000-0-AP RRID:AB_11042316	1:1000
Rabbit monoclonal anti-H4 [81]	Cell Signaling Technology	Cat# 13919 RRID:AB_2798345	1:1000
Rabbit monoclonal anti-H2A [82]	Cell Signaling Technology	Cat# 12349 RRID:AB_2687875	1:1000
Rabbit monoclonal anti-H2B [83]	Cell Signaling Technology	Cat# 12364 RRID:AB_2714167	1:1000
Rabbit polyclonal anti-Phospho-(S/T) Phe [84]	Cell Signaling Technology	Cat# 9631 RRID:AB_330308	1:1000
Rabbit polyclonal anti-Acetylated-lysine [85]	Cell Signaling Technology	Cat# 9441 RRID:AB_331805	1:1000

Rabbit polyclonal anti-pan methyl lysine [86]	Abcam	Cat# ab7315 RRID:AB_305840	1:1000
Rabbit polyclonal anti-PAR [87]	Cell Signaling Technology	Cat# 83732 RRID:AB_2749858	1:1000
Rabbit monoclonal anti-p300 [88]	Cell Signaling Technology	Cat# 86377S, RRID:AB_2800077	1:1000
Rabbit monoclonal anti-CBP [88]	Cell Signaling Technology	Cat# 7389S, RRID:AB_2616020	1:1000
Rabbit monoclonal anti-hMOF [89]	Abcam	Cat# ab200660 RRID:AB_2891127	1:1000
Rabbit polyclonal anti-PCAF [90]	Cell Signaling Technology	Cat# 3378 RRID:AB_10679933	1:1000
Rabbit anti-Tip60 [91]	Cell Signaling Technology	Cat# 12058S RRID:AB_2797811	1:1000
Rabbit polyclonal anti-PARP1 [92]	Cell Signaling Technology	Cat# 9542 RRID:AB_2160739	1:1000
Rabbit polyclonal anti-Ki67 [93]	Abcam	Cat# ab15580 RRID:AB_443209	1:1000
Normal Rabbit IgG [94]	Santa Cruz Biotechnology	Cat# 2729 RRID: AB_1031062	1:1000

Supplementary References

66 Marmolejo, C. O. *et al.* A phosphorylation code coordinating transcription condensate dynamics with DNA replication. *bioRxiv*, 2024.2005.2010.593572 (2024).

67 Ferrari, R. *et al.* TFIIIC Binding to Alu Elements Controls Gene Expression via Chromatin Looping and Histone Acetylation. *Mol Cell* **77**, 475-487 e411 (2020).

68 Yang, W. *et al.* Downregulation of lncRNA APCDD1L-AS1 due to DNA hypermethylation and loss of VHL protein expression promotes the progression of clear cell renal cell carcinoma. *Int J Biol Sci* **18**, 2583-2596 (2022).

69 Igarashi, T. *et al.* An ATR-PrimPol pathway confers tolerance to oncogenic KRAS-induced and heterochromatin-associated replication stress. *Nat Commun* **14**, 4991 (2023).

70 Nan, Y. *et al.* DLGAP1-AS2-Mediated Phosphatidic Acid Synthesis Activates YAP Signaling and Confers Chemoresistance in Squamous Cell Carcinoma. *Cancer Res* **82**, 2887-2903 (2022).

71 Zhao, B. *et al.* The molecular basis of tight nuclear tethering and inactivation of cGAS. *Nature* **587**, 673-677 (2020).

72 Ye, Q. *et al.* DTX3L-mediated TIRR nuclear export and degradation regulates DNA repair pathway choice and PARP inhibitor sensitivity. *Nat Commun* **15**, 10596 (2024).

73 Cao, D., Ma, B., Cao, Z., Zhang, X. & Xiang, Y. Structure of Semliki Forest virus in complex with its receptor VLDLR. *Cell* **186**, 2208-2218 e2215 (2023).

74 Thiele, S. *et al.* Cellular Importin-alpha3 Expression Dynamics in the Lung Regulate Antiviral Response Pathways against Influenza A Virus Infection. *Cell Rep* **31**, 107549 (2020).

75 Ferretti, S. *et al.* Discovery of WRN inhibitor HRO761 with synthetic lethality in MSI cancers. *Nature* **629**, 443-449 (2024).

76 Chen, Q. Q. *et al.* Neuraminidase 1 promotes renal fibrosis development in male mice. *Nat Commun* **14**, 1713 (2023).

77 ElGhazaly, M., Collins, M. O., Ibler, A. E. M. & Humphreys, D. Typhoid toxin hijacks Wnt5a to establish host senescence and Salmonella infection. *Cell Rep* **42**, 113181 (2023).

78 Yan, J. *et al.* Development of Aptamer-DNAzyme based metal-nucleic acid frameworks for gastric cancer therapy. *Nat Commun* **15**, 3684 (2024).

79 Sun, Z., Zhang, Z., Wang, Q. Q. & Liu, J. L. Combined Inactivation of CTPS1 and ATR Is Synthetically Lethal to MYC-Overexpressing Cancer Cells. *Cancer Res* **82**, 1013-1024 (2022).

80 Deng, H. *et al.* The WDR11 complex is a receptor for acidic-cluster-containing cargo proteins. *Cell* **187**, 4272-4288 e4220 (2024).

81 Pardo-Lorente, N. *et al.* Nuclear localization of MTHFD2 is required for correct mitosis progression. *Nat Commun* **15**, 9529 (2024).

82 Song, Z. *et al.* Regulation of hepatic inclusions and fibrinogen biogenesis by SEL1L-HRD1 ERAD. *Nat Commun* **15**, 9244 (2024).

83 Kikuchi, M. *et al.* Epigenetic mechanisms to propagate histone acetylation by p300/CBP. *Nat Commun* **14**, 4103 (2023).

84 Tu, Y. *et al.* TBC1D23 mediates Golgi-specific LKB1 signaling. *Nat Commun* **15**, 1785 (2024).

85 Tiwari, A. *et al.* Mitochondrial pyruvate transport regulates presynaptic metabolism and neurotransmission. *Sci Adv* **10**, eadp7423 (2024).

86 Tu, W. J. *et al.* Targeting novel LSD1-dependent ACE2 demethylation domains inhibits SARS-CoV-2 replication. *Cell Discov* **7**, 37 (2021).

87 Fabian, Z. *et al.* PARP1-dependent DNA-protein crosslink repair. *Nat Commun* **15**, 6641 (2024).

88 Huoh, Y. S. *et al.* Mechanism for controlled assembly of transcriptional condensates by Aire. *Nat Immunol* **25**, 1580-1592 (2024).

89 Wu, Y. *et al.* Disrupting the phase separation of KAT8-IRF1 diminishes PD-L1 expression and promotes antitumor immunity. *Nat Cancer* **4**, 382-400 (2023).

90 Malone, C. F. *et al.* The KAT module of the SAGA complex maintains the oncogenic gene expression program in MYCN-amplified neuroblastoma. *Sci Adv* **10**, eadm9449 (2024).

91 Li, M. *et al.* Epigenetic Control of Translation Checkpoint and Tumor Progression via RUVBL1-EEF1A1 Axis. *Adv Sci (Weinh)* **10**, e2206584 (2023).

92 Konig, C., Ivanisenko, N. V., Ivanisenko, V. A., Kulms, D. & Lavrik, I. N. Pharmacological targeting of caspase-8/c-FLIP(L) heterodimer enhances complex II assembly and elimination of pancreatic cancer cells. *Commun Biol* **8**, 4 (2025).

93 Chong, A. C. N. *et al.* Checkpoint kinase 2 controls insulin secretion and glucose homeostasis. *Nat Chem Biol* **20**, 566-576 (2024).

94 Yi, Y. *et al.* Mitochondrial-cytochrome c oxidase II promotes glutaminolysis to sustain tumor cell survival upon glucose deprivation. *Nat Commun* **16**, 212 (2025).